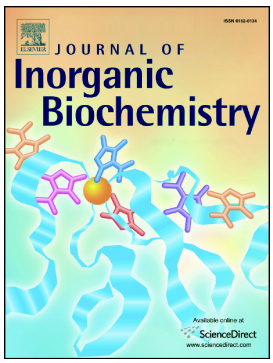

A study of the properties, reactivity and antitumor activity of novel N-methylated-3-thiazolyl or 3-thienyl carbazoles and their Pd(II) and Pt(II) complexes

M. Reig, R. Bosque, M. Font-Bardía, C. Calvis, R. Messeguer, L. Baldomà, J. Badía, D. Velasco, C. López

PII: S0162-0134(17)30799-7
DOI: doi:10.1016/j.jinorgbio.2018.03.008
Reference: JIB 10459

To appear in: *Journal of Inorganic Biochemistry*

Received date: 14 November 2017
Revised date: 14 February 2018
Accepted date: 12 March 2018

Please cite this article as: M. Reig, R. Bosque, M. Font-Bardía, C. Calvis, R. Messeguer, L. Baldomà, J. Badía, D. Velasco, C. López , A study of the properties, reactivity and antitumor activity of novel N-methylated-3-thiazolyl or 3-thienyl carbazoles and their Pd(II) and Pt(II) complexes. The address for the corresponding author was captured as affiliation for all authors. Please check if appropriate. Jib(2017), doi:10.1016/j.jinorgbio.2018.03.008

A study of the properties, reactivity and antitumor activity of novel N-methylated-3-thiazolyl or 3-thienyl carbazoles and their Pd(II) and Pt(II) complexes

M. Reig,[a] R. Bosque,[b] M. Font-Bardía,[c] C. Calvis,[d] R. Messeguer,[d] L. Baldomà,[e] J. Badía,[e] D. Velasco[a] and C. López*[b]

[a] *Grup de Materials Orgànics, Institut de Nanociència i Nanotecnologia (IN^{2}UB), Secció de Química Orgànica, Departament de Química Inorgànica i Orgànica, Facultat de Química, Martí i Franquès 1-11, E-08028 Barcelona, Spain*

[b] *Secció de Química Inorgànica, Departament de Química Inorgànica i Orgànica, Facultat de Química, Martí i Franquès 1-11, E-08028 Barcelona, Spain*

[c] *Unitat de Difracció de Raigs-X, Centres Científics i Tecnològics (CCiT), Universitat de Barcelona, Solé i Sabaris 1–3, E-08028 Barcelona, Spain*

[d] *Biomed Division LEITAT Technological Center, Parc Científic de Barcelona, Edifici Hèlix, Baldiri i Reixach 13-21, E-08028 Barcelona, Spain*

[e] *Departament de Bioquímica i Biologia Molecular, Facultat de Farmàcia, Av. Joan XXIII s/n, E-08028 Barcelona, Spain*

Keywords

Carbazole – Pd(II)-based complexes – Pt(II)-based complexes – Cancer / Antitumor activity

Abstract

The synthesis and characterization of two hybrid *N*-methylated carbazole derivatives containing a thiazolyl or a thienyl ring on position 3 is reported. The thiazolyl derivative has been also characterised by X-Ray diffraction. The study of its reactivity in front of $[MCl_2(dmso)_2]$ (M = Pd or Pt) or $Na_2[PdCl_4]$ in methanol has allowed us to isolate and characterize its complexes. However, when the reactions were performed using the thienyl analogue, no evidences of the formation of any Pd(II) or Pt(II) complex were detected. Thus indicating that the latter is less prone to bind to the M(II) ions than its thiazolyl analogue. DFT and TD-DFT calculations have also been carried out in order to: a) rationalize the influence of the nature of the thiazolyl or

thienyl group on the electronic delocalization and b) assign the bands detected in their electronic spectra. Molecular mechanics calculations show that the free rotation of the thiazolyl in relation to the carbazole requires a greater energy income than for its thienyl analogue. Comparative studies of the cytotoxic activity of the new ligands and the metal complexes on colon (HCT116) and two breast (MDA-MB231 and MCF7) cancer cell lines are also reported. In order to get additional information on mode of action of the new products, comparative studies on their potential ability to: a) modify the electrophoretic mobility of pBluescript SK^+ plasmid DNA and b) act as inhibitors of Topoisomerases I and IIα or cathepsin B have also been carried out.

1. Introduction

Cancer is among the leading causes of morbidity and death that unfortunately affects millions of persons worldwide (i.e. more than one million each year in USA [1]). The American Cancer Society estimates an incidence of ca. 1.7 million new cases for 2017 and more than 0.6 million deaths [2] mainly produced by colorectal, breast, lung and ovarian cancers [2-4]). Every cancer type needs a specific treatment protocol that usually involves chemotherapy (CT) [5], radiotherapy and/or surgery. The development of new antitumor drugs with improved activities and lower side effects than those used nowadays in CT is still one of the main challenges of current research in medicinal chemistry. Among the variety of strategies used nowadays in drug discovery [6], those with greater expectations are based on: a) natural products and/ or b) new synthetic products with several bioactive arrays (i.e. by incorporation of an additional bioactive unit in the backbones of commercially available pharmaceuticals or known drugs and commonly known as “molecular hybridization approach”) [6].

On the other hand, it is well-known that heterocycles and their derivatives are one of the most important types of organic compounds due to their outstanding physical and photo-optical properties, their rich reactivity, their utility as ligands in Coordination and Organometallic Chemistry and their multiple applications in a variety of fields, including medicinal chemistry [7-9]. Heterocyclic cores are present in huge range of natural and marketed antimicrobial, anti-

inflammatory, antiviral, anticancer, antihypertensive, antimalarial, anti-HIV, antidepressant, antihelmintic drugs, among others. Their relevance in new drugs design and development is undeniable [7]. For instance, among all the anticancer drugs approved by FDA during the late five years ca. 75% have heterocyclic arrays with N and / or S atoms or polycyclic aromatic compounds with heterocyclic fragments [8-10].

Carbazole (Fig. 1), thiazole and thiophene are probably three of the most important scaffolds in drug design and discovery [11-13]. These units are present in diverse bioactive synthetic -and even in naturally occurring products. For instance, *Ellipticine* and Glybomine-C (Fig. 1) isolated from plants, are potent cytotoxic agents in several cancer cell lines [14] and the discovery that *N*-alkylation of *Ellipticine* enhanced inhibition growth activity has stimulated the interest on *N*-substituted carbazoles [11,14]. The number of potent cytotoxic (substituted and /or anellated) carbazoles reported in the last 2 years has grown exponentially and according to a recent review published by Caruso et al. [11d]: "*Carbazoles are promising scenarios for breast cancer treatments*".

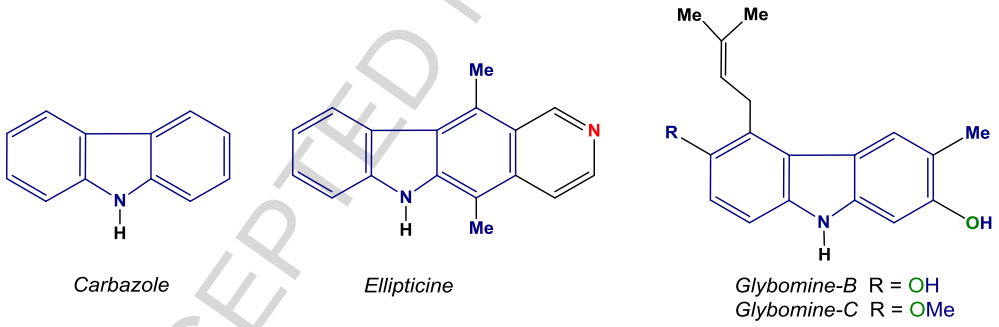

Fig. 1. Carbazole and two naturally occurring carbazole derivatives (Ellipticine and Glybomine-B and C) with potent cytotoxic activities in front of several cancer cell lines.

In addition to carbazoles, and in a lesser extent, thiazole and thiophene derivatives are gaining increasing interest as "central cores" or as "pendant" groups in drug engineering and specially as promising platforms or "templates" to build up new and more efficient antitumor agents that could overcome or at least reduce the main problems (i.e. drug resistance, toxicity, or other undesirable side effects) associated to drugs used currently. *Cis*-$[PtCl_2(NH_3)_2]$ (*cisplatin*) and *Doxorubicin* [4,15,16] are two CT agents used in cancer treatments that may generate

severe-side effects (i.e. nephrotoxicity, neurotoxicity, the increase of blood pressure, severe nausea, vomiting, or diarrhoea produced by cisplatin or severe heart problems (cardiomyopathy) associated to doxorubicin [15,16]).

Despite of the interest in electronics and materials science arisen by hybrid carbazole / thienyl derivatives [17-20] and the potential synergic effect of the presence of two bioactive arrays [i.e. the N-substituted carbazole and a thiazole (or a thienyl) unit] in the same molecule that could be relevant in drug design [21] and in photodynamic therapy (PTD) [22], studies on their biological activities are scarce. Moreover, it is well-known that heterocycles are valuable ligands in Coordination and Organometallic Chemistry [8] and their binding to a transition metal ion (M^{m+}) commonly affects their properties and their biological and / or catalytic activities. For instance, Pd(II) and Pt(II) complexes with heterocyclic ligands (i.e. pyrazoles, indoles) showing greater cytotoxic activity than the free ligands have been reported [23]. However, parallel studies on hybrid carbazole / thiazole or thiophene derivatives have not been investigated yet. Therefore, there is a lack of information on their coordination ability and the effect produced by the binding of these ions on their properties and especially on their cytotoxic activity.

In this paper, we present two new carbazole derivatives: 9-methyl-3-(2-thiazolyl)-9*H*-carbazole (**1a**) and 9-methyl-3-(2-thienyl)-9*H*-carbazole (**1b**) shown in Scheme 1, a study of their reactivity in front of Pd(II) and Pt(II), their spectroscopic properties and the antitumor activity of the free ligands and the new Pd(II) and Pt(II) complexes.

2. Experimental

2.1. Chemistry

2.1.1. Materials and methods

$[MCl_2(dmso)_2]$ (M = Pd or Pt) and 3-iodo-9*H*-carbazole were prepared as described previously [24-26], and the remaining reagents were obtained from commercial sources and used as received. The success of the synthesis of the Pt(II) compound **3a** is strongly dependent on the quality of the methanol, the presence of water produces the formation of metallic

platinum, other undesirable minor by-products and a significant decrease in the yield. Thus, the use of high quality MeOH (HPLC grade) is required. The remaining solvents used were dried and distilled before use [27]. During the preparation of the complexes (**2a** and **3a**), the reaction flask was protected from the light with aluminium foil. Elemental analysis were carried out at the *Centres Científics i Tecnològics* (CCiT, Univ. Barcelona) with an Eager 1108 microanalyzer. Mass spectra (ESI^+) were performed at the *Servei d'Espectrometria de Masses* (Univ. de Barcelona) using a LC/MSD-TOF Agilent Technologies instrument. UV-vis. spectra of CH_2Cl_2 solutions of the free ligands (**1a** and **1b**) and complexes **2a** and **3a** were recorded at 298 K with a Varian Cary UV-Vis-NIR 500E spectrometer and their emission spectra were obtained on a PTI fluorimeter equipped with a 220B lamp power supply, a 815 photomultiplier detection system and a Felix 32 software at 298 K in CH_2Cl_2 solutions. 1,4-Bis(5-phenyl-2-oxazolyl)benzene (POPOP) dissolved in cyclohexane was used as a standard for the fluorescence quantum yield determination (λ_{exc} = 300 nm, Φ_{POPOP} =0.93). ^1H and $^{13}C\{^1H\}$-NMR spectra were recorded at 298 K in acetone-d_6 for the precursor (3-iodo-9-methyl-9*H*-carbazole) or in $CDCl_3$ (in the remaining cases) with a Varian Mercury 400 MHz and a Bruker 400 MHz Avance III [for ^1H and $^{13}C\{^1H\}$] and a Bruker 250 MHz and a Bruker 400 Avance III HD (for $^{195}Pt\{^1H\}$) spectrometers. Chemical shifts are given in δ values (ppm) using the solvent peaks as internal references (^1H and ^{13}C) and H_2PtCl_6 in D_2O ($^{195}Pt\{^1H\}$) and coupling constants (J) are given in Hz. Abbreviations used for the multiplicities are as follows: s (singlet), d (doublet), dd (doublet of doublets), t (triplet), q (quadruplet) and m (multiplet). The atom numbering system used in the assignment of ^1H and $^{13}C\{^1H\}$-NMR data is shown in Chart 1.

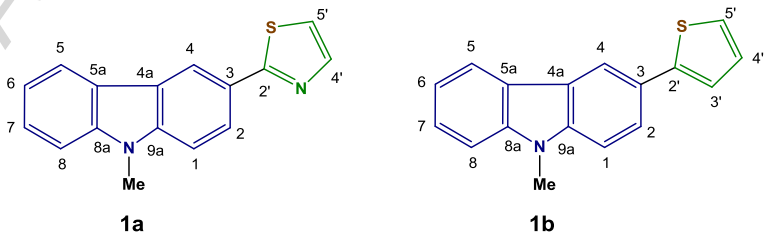

Chart 1. Atom labelling scheme for ligands **1a** and **1b**.

*2.1.2. Synthesis of ligands **1a** and **1b***

2.1.2.1. Synthesis of the precursor 3-iodo-9-methyl-9H-carbazole. NaH (240 mg, 6.00×10^{-3} mol, 60% dispersion in mineral oil) was added to a solution of 3-iodo-9*H*-carbazole (1.60 g, 5.46×10^{-3} mol) in anhydrous DMF (10 mL) under nitrogen atmosphere. The solution was stirred at room temperature for 30 minutes. Then, iodomethane (374 µL, 6.00×10^{-3} mol) was added and the mixture was stirred at room temperature for 30 minutes and then treated with water. The aqueous layer was extracted with CH_2Cl_2 and the organic layer was dried over Na_2SO_4, filtered off and the solvent was distilled off under reduced pressure. The crude was purified by flash column chromatography using a mixture of hexane and ethyl acetate (20 : 1 v/v) as the eluent to give 3-iodo-9-methyl-9*H*-carbazole (1.45 g, 86%). ^{1}H NMR (400 MHz, acetone-d_6) δ (ppm): 8.49 (d, $^4J_{H\text{-}H}$ = 1.7, 1H, H^4), 8.17 (d, $^3J_{H\text{-}H}$ = 7.6, 1H, H^5), 7.74 (dd, $^3J_{H\text{-}H}$ = 8.6, $^4J_{H\text{-}H}$ = 1.7, 1H, H^2), 7.55 (d, $^3J_{H\text{-}H}$ = 8.2, 1H, H^8), 7.53-7.48 (m, 1H, H^7), 7.42 (d, $^3J_{H\text{-}H}$ = 8.6, 1H, H^1), 7.26-7.22 (m, 1H, H^6), 3.91 (s, NMe, 3H). CI-MS (m/z): calc. for $C_{13}H_{11}IN$ $(M + H)^+$ 308.0, found: 308.0.

*2.1.2.2. Synthesis of 9-methyl-3-(2-thiazolyl)-9H-carbazole (**1a**)*. A mixture of 9-methyl-3-iodo-9*H*-carbazole (1.24 g, 4.04×10^{-3} mol), 2-(tributylstannyl)thiazole (1.81 g, 4.84×10^{-3} mol) and $Pd(PPh_3)_4$ (231 mg, 0.20×10^{-3} mol) in anhydrous DMF (10 mL) was heated to 100 °C under a nitrogen atmosphere for 20 h. Then, the reaction mixture was cooled down to room temperature, treated with water and the product was extracted with dichloromethane. The organic layer was dried over Na_2SO_4, filtered off and the solvent was distilled off under reduced pressure. The crude was purified by flash column chromatography using a mixture of hexane and CH_2Cl_2 (5 : 1 v/v) as the eluent to give compound **1a** (420 mg, 39%). ^{1}H NMR (400 MHz, $CDCl_3$) δ (ppm): 8.73 (d, $^4J_{H\text{-}H}$ = 1.7, 1H, H^4), 8.16 (d, $^3J_{H\text{-}H}$ = 8.0, 1H, H^5), 8.10 (dd, $^3J_{H\text{-}H}$ = 8.6 , $^4J_{H\text{-}H}$ = 1.7 Hz, 1H, H^2), 7.87 (d, $^3J_{H\text{-}H}$ = 3.3, 1H, $H^{4'}$), 7.54-7.50 (m, 1H, H^7), 7.44 (d, $^3J_{H\text{-}H}$ = 8.6, 1H, H^1), 7.43 (d, $^3J_{H\text{-}H}$ = 8.2, 1H, H^8), 7.31-7.27 (m, 2H, H^6 and $H^{5'}$), 3.89 (s, 3H, NMe). ^{13}C NMR (100 MHz, $CDCl_3$) δ (ppm): 170.0 ($C^{2'}$), 143.4 ($C^{4'}$), 142.2 (C^{9a}), 141.7 (C^{8a}), 126.5 (C^7), 125.1 (C^3), 124.9 (C^2), 123.3 (C^{4a}), 123.0 (C^{5a}), 120.8 (C^5), 119.7 (C^6), 119.0 (C^4), 117.8 ($C^{5'}$), 108.9 (2C, C^1 and C^8), 29.4 (N-

CH_3). HRMS (ESI-MS) (m/z): calc. for $C_{16}H_{13}N_2S$ $(M + H)^+$: 265.0794, found: 265.0796. Elemental Anal. (%). Calc. for $C_{16}H_{12}N_2S$ (MW = 264.34). C, 72.70; H, 4.58; N, 10.60 and S, 12.13; found: C, 72.65; H, 4.65; N, 10.53; and S, 11.86.

*2.1.2.3. Synthesis of 9-methyl-3-(2-thienyl)-9H-carbazole (**1b**).* A mixture of 9-methyl-3-iodo-9*H*-carbazole (771 mg, 2.51×10^{-3} mol), 2-(tributylstannyl)thiophene (1.12 g, 3.00×10^{-3} mol) and $Pd(PPh_3)_4$ (139 mg, 0.12×10^{-3} mol) in anhydrous DMF (10 mL) was heated to 100 °C under a nitrogen atmosphere for 24 h. Then, the reaction mixture was cooled down to room temperature, treated with water and the product was extracted with dichloromethane. The organic layer was dried over Na_2SO_4, filtered off and the solvent was distilled off under reduced pressure. The crude was purified by flash column chromatography using a mixture of hexane and dichloromethane (9 : 1 v/v) as the eluent to give compound **1b** (343 mg, 52%). ^{1}H NMR (400 MHz, $CDCl_3$) δ (ppm): 8.32 (d, $^4J_{H\text{-}H}$ = 1.8, 1H, H^4), 8.14 (d, $^3J_{H\text{-}H}$ = 7.7, 1H, H^5), 7.75 (dd, $^3J_{H\text{-}H}$ = 8.5 Hz, $^4J_{H\text{-}H}$ = 1.8, 1H, H^2), 7.52-7.48 (m, 1H, H^7), 7.41 (d, $^3J_{H\text{-}H}$ = 8.1, 1H, H^8), 7.40 (d, $^3J_{H\text{-}H}$ = 8.5 Hz, 1H, H^1), 7.35 (dd, $^3J_{H\text{-}H}$ = 3.6, $^4J_{H\text{-}H}$ = 1.0, 1H, $H^{3'}$), 7.28-7.24 (m, 2H, $H^{5'}$ and H^6), 7.11 (dd, $^3J_{H\text{-}H}$ = 5.1, $^3J_{H\text{-}H}$ = 3.6, 1H, $H^{4'}$), 3.87 (s, 3H, NMe). ^{13}C NMR (100 MHz, $CDCl_3$) δ (ppm): 146.0 ($C^{2'}$), 141.6 (C^{8a}), 140.7 (C^{9a}), 128.1 ($C^{4'}$), 126.2 (C^7), 125.9 (C^3), 124.5 (C^2), 123.8 ($C^{5'}$), 123.3 (C^{4a}), 122.9 (C^{5a}), 122.2 ($C^{3'}$), 120.6 (C^5), 119.3 (C^6), 118.0 (C^4), 108.9 (C^1 or C^8), 108.8 (C^1 or C^8), 29.4 (NMe). HRMS (ESI-MS) (m/z): calc. for $C_{17}H_{14}NS$ $(M + H)^+$ 264.0841, found: 264.0843; elemental Anal (%). Calc. for $C_{17}H_{13}NS$ (MW = 263.34). C, 77.53; H, 4.98; N, 5.32 and S, 12.70; found: C, 72.45; H, 5.04; N, 5.25; and S, 12.61.

*2.1.3. Preparation of the complexes **2a** and **3a***

*2.1.3.1. Synthesis of compound **2a**.* This compound was obtained using two alternative procedures that differ in the nature of the starting Pd(II) complex used as reagent: $[PdCl_2(dmso)_2]$ or $Na_2[PdCl_4]$ {methods *a)* and *b)*, respectively}. Method *b*) allows the isolation of compound **2a** with a higher yield (and at lower temperatures) than using method *a*).

Method a) [$PdCl_2(dmso)_2$] (63 mg, 1.9×10^{-4} mol) was treated with 30 mL of methanol, refluxed until complete dissolution and filtered out. Then, 50 mg (1.9×10^{-4} mol) of carbazole **1a**, were added to the hot filtrate and the mixture was refluxed for 1 h. After this period, the resulting solution was allowed to cool down to room temperature and the solid formed was collected by filtration, air-dried and later on dried in vacuum for 2 days. (Yield: 38 mg, 57 %).

Method b) A solution containing $Na_2[PdCl_4]$ (28 mg, 9.5×10^{-5} mol) and 20 mL of methanol was added to another one formed by ligand **1a** (50 mg, 1.9×10^{-4} mol) and 5 mL of methanol. The resulting mixture was stirred for 24 h at 298 K. After this period, the solid formed was collected by filtration and dried as in *Method a)* (Yield: 55 mg, 82 %). ^{1}H NMR (400 MHz, $CDCl_3$) δ (ppm): 9.22 (d, $^4J_{H\text{-}H}$ = 1.8, 2H, 2H^4), 8.47 (dd, $^3J_{H\text{-}H}$ = 8.5, $^4J_{H\text{-}H}$ = 1.8, 2H, 2H^2), 8.19 (d, $^3J_{H\text{-}H}$ = 7.7, 2H, 2H^5), 8.08 (d, $^3J_{H\text{-}H}$ = 3.7, 2H, 2H$^{4'}$), 7.58-7.44 (m, 8H, 2H^1, 2H^7, 2H^8 and 2H$^{5'}$), 7.32 (t, $^3J_{H\text{-}H}$ = 7.7, 2H, 2H^6), 3.93 (s, 6H, 2NMe). Elemental Anal. (%). Calc. for $C_{32}H_{24}Cl_2N_4PdS_2$ (MW = 706.01). C, 54.44; H, 3.43; N, 7.94 and S, 9.08; found: C, 54.50; H, 3.50; N, 8.03 and S, 8.85.

*2.1.3.2. Synthesis of compound **3a**. cis*-[$PtCl_2(dmso)_2$] (80 mg, 1.9×10^{-4} mol) was suspended in 30 mL of methanol, until complete dissolution. Then, the hot solution was filtered out and the filtrate was poured into a methanol solution (5 mL) of ligand **1a** (50 mg, 1.9×10^{-4} mol). The reaction flask was protected from light with aluminium foil and the mixture was refluxed for 1 h and filtered. Then, the filtrate was afterwards concentrated to dryness on a rotary evaporator and the residue was dried in vacuum for 24 h. After this period, the solid was dissolved in the minimum amount of CH_2Cl_2 (ca. 15 mL) and passed through a short SiO_2 column (5.0 cm $\times$ 1.5 cm). Elution with CH_2Cl_2 released a pale yellowish band that was collected and concentrated to dryness on a rotary evaporator giving **3a** (yield: 69 mg, 60 %). ^{195}Pt{^{1}H}-NMR data (54 MHz, $CDCl_3$) δ (ppm): -2983 (s). ^{1}H NMR-data (400 MHz, $CDCl_3$) δ (ppm): 9.22 (d, $^4J_{H\text{-}H}$ = 1.8, 1H, H^4), 8.47 (dd, $^3J_{H\text{-}H}$ = 8.5, $^4J_{H\text{-}H}$ = 1.8, 1H, H^2), 8.20 (d, $^3J_{H\text{-}H}$ = 7.7, 1H, H^5), 8.08 (d, $^3J_{H\text{-}H}$ = 3.7, 1H, H$^{4'}$), 7.58-7.54 (m, 2H, H^1 and H^7), 7.47 (d, $^3J_{H\text{-}H}$ = 8.2, 1H, H^8), 7.46 (d, $^3J_{H\text{-}H}$ = 3.7, 1H, H$^{5'}$),

7.34-7.30 (m, 1H, H^6), 3.94 (s, 3H, NMe), 3.37 (s, 6H, dmso). ESI-MS (m/z): calc. for $C_{18}H_{19}Cl_2N_2OPtS_2$ $(M + H)^+$ 608.0, found: 608.0. Elemental Anal. (%). Calc. for: $C_{18}H_{18}Cl_2N_2OPtS_2$ (MW = 608.46): C, 35.53; H, 2.98; N, 4.60 and S, 10.54; found C, 35.59; H, 3.05; N, 4.63 and S, 10.60.

*2.1.3.3. Synthesis of the two isomers of [$PtCl_2$(**1a**)(dmso)] {trans-(**3a**) and cis-(**4a**)}.* NaAcO (16 mg, 1.9×10^{-4} mol) was dissolved in 5 mL of methanol at 298 K and then added dropwise to a mixture formed by carbazole **1a** (50 mg, 1.9×10^{-4} mol), *cis*-[$PtCl_2(dmso)_2$] (80 mg, 1.9×10^{-4} mol) and 25 mL of toluene. The flask was protected from the light with aluminium foil and refluxed for 3 days. After this period the deep brown solution was filtered through a Celite pad, and the filtrate was concentrated on a rotary evaporator. The dark residue was dried in vacuum for 24 h, dissolved in CH_2Cl_2 (ca. 30 mL) and finally passed through a short (5.0 cm $\times$ 1.5 cm) SiO_2 column. Elution with CH_2Cl_2 released a wide pale yellow band that was collected in portions (ca. 25 mL / each). The first collected fractions ca. 120 mL gave after concentration 11 mg of **3a**; while the remaining subsequent fractions eluted (ca. 200 mL) gave, after concentration a solid (26 mg) containing isomers **3a** and **4a** in a ca. equimolar ratio. %). $^{195}Pt\{^1H\}$-NMR data (54 MHz, $CDCl_3$, see also Fig. S1, A) δ (ppm): -2980 (s) (*trans*- isomer, **3a**) and -2932 (s) (*cis*- isomer, **4a**); ^1H NMR data (400 MHz, $CDCl_3$) δ (ppm): (see also Fig. S1, **B**): 9.22 (d, $^4J_{H\text{-}H}$ = 1.8, 1H, H^4 of **3a**), 8.47 (dd, $^3J_{H\text{-}H}$ = 8.5 , $^4J_{H\text{-}H}$ = 1.8 , 1H, H^2 of **3a**), 8.20 (d, $^3J_{H\text{-}H}$ = 7.7, 1H, H^5 of **3a**), 8.08 (d, $^3J_{H\text{-}H}$ = 3.7 , 1H, $H^{4'}$ of **3a**), 7.58-7.54 (m, 2H, H^1 and H^7 of **3a**), 7.47 (d, $^3J_{H\text{-}H}$ = 8.2, 1H, H^8 of **3a**), 7.46 (d, $^3J_{H\text{-}H}$ = 3.7 , 1H, $H^{5'}$), 7.34-7.30 (m, 1H, H^6 of **3a**), 3.98 (s, 3H, NMe of **4a**); 3.94 (s, 3H, NMe of **3a**), 3.37 (s, 6H, Me(dmso) of **3a**); 3.25 [s, 3H, Me(dmso) of **4a**]; and 2.29 [s, 3H, Me(dmso) of **4a**]. ESI-MS (m/z): calc. for $C_{18}H_{19}Cl_2N_2OPtS_2$ $(M + H)^+$ = 608.0; found: 608.0. Elemental Anal. (%). Calc. for: $C_{18}H_{18}Cl_2N_2OPtS_2$ (MW = 608.46): C, 35.53; H, 2.98; N, 4.60 and S, 10.54; found C, 35.59; H, 3.15; N, 4.54 and S, 10.37.

2.2. Crystallography

A colourless prism-like specimen of $C_{16}H_{12}N_2S$ (**1a**) (sizes in Table 1) was used for the X-ray crystallographic analysis. The X-ray intensity data were measured on a D8 Venture system equipped with a multilayer monochromator and a Mo microfocus (λ = 0.71073 Å). The frames were integrated with the Bruker SAINT software package using a narrow-frame algorithm. The integration of the data using an orthorhombic unit cell yielded a total of 7259 reflections to a maximum θ angle of 27.50° (0.77 Å resolution), of which 2855 were independent (average redundancy 2.543, completeness = 99.9%, R_{int} = 3.42%, R_{sig} = 4.25%) and 2482 (86.94%) were greater than $2\sigma(F^2)$. The final cell constants given in Table 1 are based upon the refinement of the XYZ-centroids of reflections above 20 σ(I). The calculated minimum and maximum transmission coefficients (based on crystal size) are 0.6711 and 0.7456. The structure was solved using the Bruker SHELXTL Software Package, and refined using SHELXL [28], using the space group $P2_12_12_1$, with Z = 4 for the formula unit, $C_{16}H_{12}N_2S$. The final anisotropic full-matrix least-squares refinement on F^2 with 173 variables converged at R_1 = 3.58%, for the observed data and wR_2 = 8.01% for all data. The goodness-of-fit was 1.074. The largest peak in the final difference electron density synthesis was 0.241 e-/Å^3 and the largest hole was -0.234 e-/Å^3 with an RMS deviation of 0.053 e$^-$/Å^3. Further details concerning the resolution and refinement of the crystal structure are presented in Table 1. CCDC-1560144 contains the crystallographic data of this paper. These data can be obtained from the *Cambridge Crystallographic Data Centre* via: www.ccdc.cam.ac.uk/data.request.cif

Table 1. Crystal data and details of the refinement for compound **1a**.

Empirical formula	$C_{16}H_{12}N_2S$
Formula weight	264.34
Temperature / K	100(2)
λ / Å	0.71073
Crystal sizes / mm× mm × mm	0.292 × 0.168 × 0.048
Crystal system	Orthorhombic
Space group	$P2_12_12_1$
a / Å	6.0702(2)
b / Å	12.8577(5)
c / Å	16.0721(6)
$\alpha = \beta = \gamma$ / deg.	90
V / Å^3	1254.41(8)
Z	4
Density (calculated)/ Mg×m^{-3}	1.400
μ / mm^{-1}	0.243
F(000)	552
Θ range for data collection / deg.	from 2.028 to 27.498
Index ranges	$-7 \le h \le 7$, $-16 \le k \le 16$, $-20 \le l \le 20$
Completeness to Θ = 25.242°	99.9 %
Absorption correction	Semi-empirical from equivalents
Max. and min. transmission	0.7456 and 0.6711
Refinement method	Full-matrix least-squares on F^2
Data / restraints / parameters	2855 / 0 / 173
Goodness-of-fit on F2	1.074
Final R indices [I >2σ(I)]	$R^1 = 0.0358$, $wR_2 = 0.0743$
R indices (all data)	$R_1 = 0.0471$, $wR_2 = 0.0801$
Absolute structure parameter	0.04(4)
Largest diff. peak and hole/ e.Å^{-3}	0.241 and -0.234

2.3. Computational details

The conformational map has been searched at the molecular mechanics level using the augmented MMFF94 method [29] as implemented in Spartan [30]. The dihedral angle S1-C2-C3-C4 (φ) has been sampled every 5 deg. and the remaining geometric parameters have been

fully optimized. DFT [31] calculations have been performed using the B3LYP functional [32,33] implemented in the Gaussian 03 software [34] and the 6-31G* basis set [35], including polarization functions for the non-hydrogen atoms.

2.4. Biological Studies

2.4.1. Cell culture

Colon adenocarcinoma (HCT116) cells (from the *American Type Culture Collection*) and breast cancer (MDA-MB231 and MCF7) cells (from *European Collection of Cell Cultures*, ECACC) were used for all the experiments. Cells were grown as a monolayer culture in minimum essential medium (DMEM with L-glutamine, without glucose and without sodium pyruvate) in the presence of 10 % heat-inactivated fetal calf serum, 10 mM of D-glucose and 0.1% streptomycin/penicillin in standard culture conditions.

2.4.2. Cell viability assays

For these studies, compounds were dissolved in 100 % DMSO at 50 mM as stock solution; then, serial dilutions have been done in DMSO (1:1) (in this way DMSO concentration in cell media was always the same); finally, 1:500 dilutions of the serial dilutions of compounds on cell media were done. The assay was carried out as described by Givens *et al*. [36]. In brief, MDA-MB231 and MCF7 cells were plated at 5000 cells/well or 10000 cells/well respectively, in 100 µL media in tissue culture 96 well plates (Cultek). After 24 h, medium was replaced by 100 µL/well of serial dilution of drugs. Each point concentration was run in triplicate. Reagent blanks, containing media plus colorimetric reagent without cells were run on each plate. Blank values were subtracted from test values and were routinely 5-10 % of uninhibited control values. Plates were incubated for 72 h. Hexosamidase activity was measured according to the following protocol: the media containing the cells was removed and cells were washed once with PBS 60 µL of substrate solution (p-nitrophenol-N-acetyl-β-D-glucosamide 7.5 mM [Sigma N-9376], sodium citrate 0.1 M, pH = 5.0, 0.25 % Triton X-100) was added to each well and incubated at 37 °C for 1-2 hours; after this incubation time, a bright yellow colour appeared; then, plates could

be developed by adding 90 µL of developer solution (Glycine 50 mM, pH = 10.4; EDTA 5 mM), and absorbance was recorded at 410 nm.

2.4.3. DNA migration studies

A stock solution (10 mM) of each compound was prepared in high purity DMSO. Then, serial dilutions were made in MilliQwater (1:1). Plasmid pBluescript SKþ (Stratagene) was obtained using a QIAGEN plasmid midi kit as described by the manufacturer. Interaction of drugs with pBluescript SK^+ plasmid DNA was analysed by agarose gel electrophoresis following a modification of the method described by Abdullah *et al.* [37]. PlasmidDNA aliquots (40 mg/mL) were incubated in TE buffer (10 mM TrisHCl, 1 mM EDTA, pH 7.5) with different concentrations of compounds **1a**, **1b, 2a** and **3a** ranging from 0 µM to 200 µM at 37 °C for 24 h. Final DMSO concentration in the reactions was always lower than 1%. For comparison, cisplatin and ethidium bromide (EB) were used as reference controls. Aliquots of 20 mL of the incubated solutions of compounds containing 0.8 mg of DNA were subjected to 1% agarose gel electrophoresis in TAE buffer (40 mM Trisacetate, 2 mM EDTA, pH 8.0). The gel was stained in TAE buffer containing ethidium bromide (ET, 0.5 mg/mL) and visualized and photographed under UV light.

2.4.4. DNA Topoisomerase I and Topoisomerase IIα inhibition assays

Topoisomerase I-based experiments were performed as described previously [38]. Supercoiled pBluescript DNA, obtained as described above, was treated with Topoisomerase I in the absence or presence of increasing concentrations of compounds **1a, 1b** and **2a**. Assay mixtures contained supercoiled pBluescript DNA (0.8 µg), calf thymus Topoisomerase I (3 units) and compounds **1a**, **1b** or **2a** (0–200 µM) in 20 µL of relaxation buffer Tris-HCl buffer (pH 7.5) containing 175 mM KCl, 5 mM $MgCl_2$ and 0.1 mM EDTA. Ethidium bromide (EB, 10 µM) was used as a control of intercalating agents and etoposide (E, 100 µM) as a control of the non-intercalating agent. Reactions were incubated for 30 min at 37 °C and stopped by the addition of 2 µL of agarose gel loading buffer. Samples were then subjected to electrophoresis and DNA bands stained with ethidium bromide as described above.

To distinguish whether compounds act as Topoisomerase inhibitors or DNA intercalators the conversion of relaxed DNA to a supercoiled state caused by the compounds was analysed in the presence of Topoisomerase I. Relaxed DNA was obtained by incubation of supercoiled DNA with Topoisomerase I as described above. Assay mixtures (20 µL) contained: relaxed DNA, Topoisomerase I (3 units) and compound (50 µM or 100 µM). Reactions were incubated 20 min at 37 °C and stopped as described above. Ethidium bromide (10 µM) was used as a control of intercalative drug.

The DNA Topoisomerase IIα inhibitory activity of the compounds tested in this study was measured as follows. Supercoiled pBluescript DNA was incubated with Topoisomerase IIα (Affymetrix) in the absence or presence of increasing concentrations of compounds under analysis. Assay mixtures contained supercoiled pBluescript DNA (0.3 µg), Topoisomerase IIα (4 units) and the tested compounds (0 - 100 µM) in 20 µL of 1x Topo II reaction buffer (PN73592). Etoposide was used as a control of Topo IIα inhibitor. Reactions were incubated for 45 min at 37 °C and stopped by the addition of 2 µL of agarose gel loading buffer. Samples were then subjected to electrophoresis and DNA bands stained with ethidium bromide as described before.

2.4.5. Cathepsin B inhibition assay

The colorimetric cathepsin B assay was performed as described by Casini *et al*. [39] with few modifications. Briefly, the reaction mixture contained 100 mM sodium phosphate (pH 6.0), 1 mM EDTA and 200 µM sodium N-carbobenzoxy-L-lysine p-nitrophenyl ester as the substrate.

To have the enzyme catalytically active before each experiment the cysteine in the active site was reduced by treatment with dithiothreitol (DTT). For this purpose, 5 mM DTT was added to the cathepsin B sample, before dilution, and incubated 1 h at 30 °C. To test the inhibitory effect of the compounds on cathepsin B, activity measurements were performed in triplicate using fixed concentrations of enzyme (500 nM) and substrate (200 µM). The compounds were used at concentrations ranging from 5 to 100 µM. Previous to the addition of substrate, cathepsin B was incubated with the different compounds at 25 °C for 2 h. The cysteine proteinase inhibitor E-64 was used as a positive control of cathepsin B inhibition. Complete

inhibition was achieved at 10 μM concentration of E-64. Activity was measured over 90 s at 326 nm on a UV-spectrophotometer.

3. Results and discussion

3.1. Synthesis and characterization

3.1.1. Synthesis of the ligands

The new carbazole derivatives: 9-methyl-3-(2-thiazolyl)-9*H*-carbazole (**1a**) and 9-methyl-3-(2-thienyl)-9*H*-carbazole (**1b**) were prepared from commercially available carbazole in a three-step-sequence of reactions (Scheme 1), that involved the iodination of the 9*H*-carbazole [26] followed by the alkylation to produce the iodo-9-methyl-9*H*-carbazole [40], that later on reacted with either 2-(tributylstannyl)thiazole (for **1a**) [41] or 2-(tributylstannyl)thiophene (for **1b**) via Stille coupling reaction [42] to produce the final products. All compounds were entirely characterized by ^{1}H NMR and ^{13}C{^{1}H} NMR spectroscopies, mass spectrometry and elemental analyses.

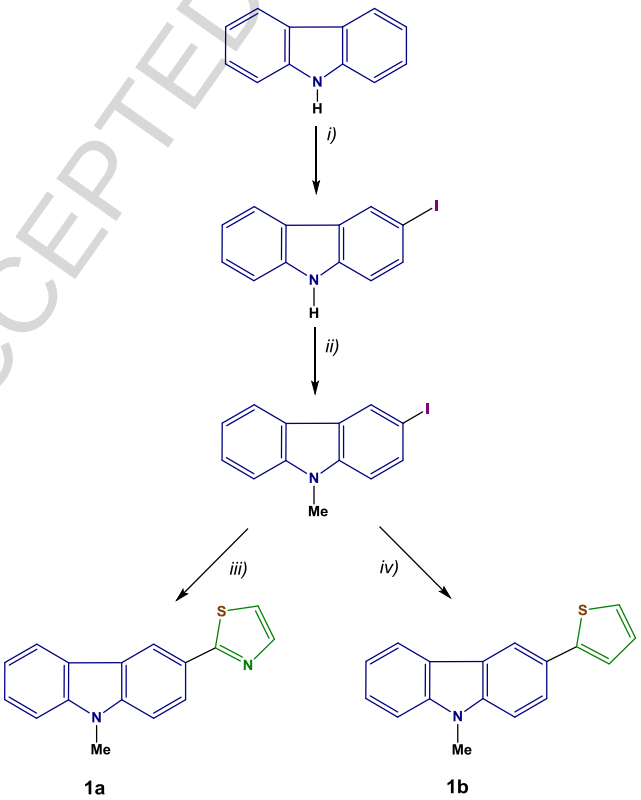

1a **1b**

Scheme 1. Synthesis of carbazoles **1a** and **1b**. Reagents and conditions: *i)* KI, KIO_3, acetic acid, reflux. *ii)* NaH, DMF, room temperature followed by treatment with iodomethane, in DMF at room temperature. *iii)* 2-(Tributylstannyl)thiazole, $[Pd(PPh_3)_4]$, DMF, 100 °C. *iv)* 2-(Tributylstannyl)thiophene, $[Pd(PPh_3)_4]$, DMF, 100 °C.

The crystal structure of compound **1a** (Fig. 2) confirmed the presence of the thiazolyl group on position 3. In compound **1a**, the nitrogen atom of the thiazolyl unit (N1) is on the same side as the Me group. As a consequence of this arrangement of groups, the N1 atom is proximal to the hydrogen atom H12 of the carbazole unit while the S1 atom is relatively close to the H4 atom. The distances N1···H12 (2.580 Å) and S1···H4 (2.751 Å) are smaller than the sum of the van der Waals radii of the atoms involved (N, 1.55 Å; H, 0.95 Å and S, 1.85 Å) [43,44]. Thus suggesting the existence of non-conventional C-H···N and C-H···S intramolecular hydrogen bonds [45], similar to those found in most 2-phenylthiazole derivatives [43,46].

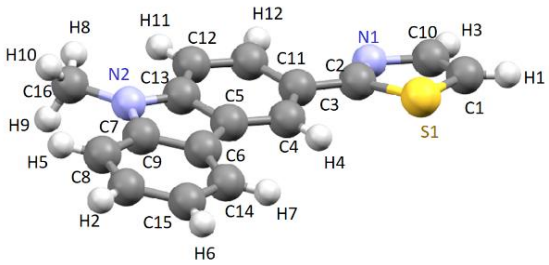

Fig. 2. Molecular structure and atom labelling scheme for the new hybrid carbazole-thiazole ligand (**1a**).

The thiazolyl group is planar and slightly twisted (ca. 13.9°) in relation to the main plane of the carbazole array. In the crystal, the relative orientation of the molecules (Fig. 3, **A**) allows π···π interactions between the heterocyclic array of a unit at (x,y,z) and the substituted phenyl ring of another one at (1+x, y, z) (the distance between the centroids of these rings is 3.90 Å). In addition, one of the hydrogen atoms of the methyl group is at only 2.77 Å from the centroid of the phenyl ring of a parallel unit, indicating the existence of intermolecular C-H···π contacts. As a consequence of this, the assembly of the molecules results in pillars (Fig. 3, **A**). These structural units are connected by additional C-H···π short contacts (Fig. 3, **B**) involving the H3 atom of the heterocyclic units in one of the pillars and the centroids of the thiazolyl groups of another one.

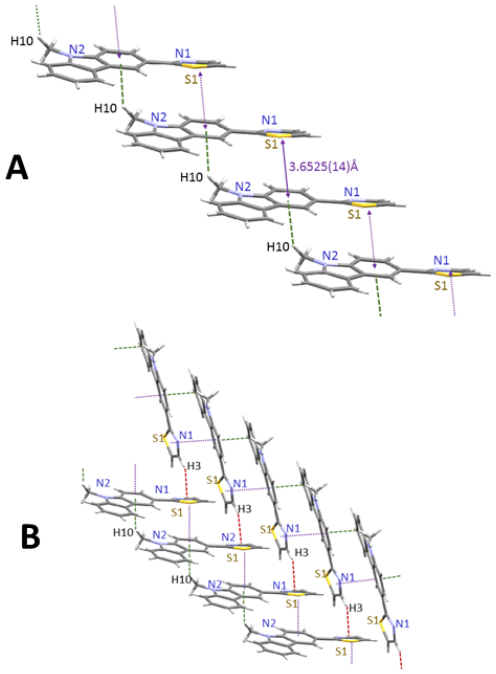

Fig. 3. Schematic view of: **A**) the assembly of a molecule of **1a**, sited at (x, y, z) and another unit at (-1+ x, y, z) by π-π stacking between the thiazolyl and the phenyl ring of the carbazole (in purple) and C-H···π short contacts (green dotted lines) involving one of the methyl protons (H10) and the propagation of these interactions along the crystal to give pillars; **B**) simplified view of connectivity of the pillars through C-H···π contacts.

*3.1.2. Coordination capability of the new hybrid carbazoles **1a** and **1b***

In view of their potential biological activities (i.e. antitumor, antibacterial), we decided to evaluate the coordination abilities of the new carbazoles in front of the Pd(II) and Pt(II) ions. In a first stage, we selected ligand **1a** and studied its reactivity with $[MCl_2(dmso)_2]$ (M = Pd or Pt) or $Na_2[PdCl_4]$ under different experimental conditions [Table 2 (entries *I-VI*) and Scheme 2]. When $[PdCl_2(dmso)_2]$ was treated with ligand **1a** [in molar ratios Pd(II): **1a** = 1 or 2] in refluxing methanol for 1 h a pale yellowish precipitate (hereinafter referred to as **2a**) was formed with a yield of 57% in the case of using a molar ratio of 1:1 (Table 2, entry *I*). Elemental analyses of **2a** and NMR characterization agreed with those expected for $[PdCl_2(\mathbf{1a})_2]$. Compound **2a** is a stable solid at room temperature and exhibits low solubility in $CHCl_3$ or CH_2Cl_2. Compound **2a** can be obtained with a higher yield of 82% and at room temperature using $Na_2[PdCl_4]$, instead of the $[PdCl_2(dmso)_2]$, a two-fold excess of carbazole **1a** and methanol as solvent (Table 2, entry *II*).

Table 2. Summary of experimental conditions [reagents, molar ratios (**1a**:Pd(II) or **1a**:Pt(II)), solvents, temperature (T), reaction time (*t,* in h)] used in the study of the reactivity of carbazole **1a** with $[PdCl_2(dmso)_2]$, $Na_2[PdCl_4]$ or *cis*-$[PtCl_2(dmso)_2]$.

Entry	Reagents	molar ratios	Solvent	T	*t*	Final products
I	**1a** : $[PdCl_2(dmso)_2]$	(1:1) or (2:1)	MeOH	reflux	1	**2a**
II	**1a** : $Na_2[PdCl_4]$	(1:1) or (2:1)	MeOH	298 K	24	**2a**
III	**1a** : *cis*-$[PtCl_2(dmso)_2]$	(1:1)	MeOH	reflux	1	**3a**
IV	**1a** : *cis*-$[PtCl_2(dmso)_2]$	(1:1)	MeOH	reflux	24	**3a**
V	**1a** : *cis*-$[PtCl_2(dmso)_2]$: NaOAc	(1:1:1)	Toluene /MeOH[a]	reflux	24	**3a** and **4a**[b]
VI	**1a** : *cis*-$[PtCl_2(dmso)_2]$: NaOAc	(1:1:1)	Toluene /MeOH[a]	reflux	72	**3a** and **4a** [c]

[a] A 5:1 mixture. [b] Only traces of compound **4a** were detected. [c] Integration of the signals observed in the ^{1}H-NMR spectrum of the raw material indicated that the molar ratio **3a**:**4a** was 1.7.

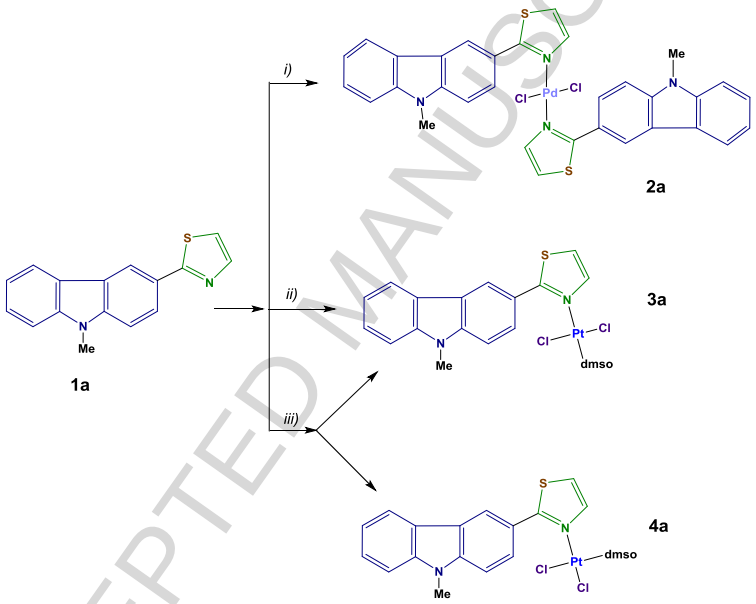

Scheme 2. Synthesis of the complexes. Reagents and conditions: *i)* $[PdCl_2(dmso)_2]$ in refluxing methanol (1 h) or $Na_2[PdCl_4]$ in methanol at 298 K, 24 h [molar ratios Pd(II):**1a** = 1:1 and 1:2, respectively]; *ii) cis*-$[PtCl_2(dmso)_2]$ in refluxing methanol (1 h) and *iii)* equimolar amounts of *cis*-$[PtCl_2(dmso)_2]$ and NaOAc in a toluene: MeOH (5:1) mixture under reflux {see text and Table 2, (entries *V* and *VI*)}.

In order to compare the effect of the binding of the M(II) ion to the carbazole **1a** on the antitumor activity, we also studied the reactivity of **1a** in front of Pt(II). Treatment of equimolar amounts of **1a** and *cis*-$[PtCl_2(dmso)_2]$ in methanol (HPLC grade) under reflux for 1 h, followed by the work-up of a SiO_2 column chromatography gave a yellowish solid (**3a**) (Table 2, entry *III* and Scheme 2). Its elemental analyses were consistent with those expected for $[PtCl_2$(**1a**)(dmso)].

Moreover, the position of the singlet observed in the $^{195}Pt\{^{1}H\}$-NMR spectrum of **3a** (δ = -2983 ppm) agrees with those of related Pt(II) complexes with a "$PtCl_2(N_{heterocycle})(S_{dmso})$" core [23b-d,47]. Its ^{1}H-NMR spectrum (Fig. S2) showed two singlets of relative intensities 1:2 in the high field region. The less intense one is assigned to the methylic protons of the ligand at δ = 4.0 ppm; while the other corresponds to the six protons of the dmso ligand. This finding is characteristic of *trans*- isomers of [$PtCl_2$(N-donor ligand)(dmso)] [23b-d,47], thus indicating that compound **3a** is *trans*-[$PtCl_2$(**1a**)(dmso)]. It should be noted that when the reaction was performed using longer reaction times no evidences of the formation of any other Pt(II) compound were detected by ^{1}H-NMR.

Since it is well-known that the presence of a base such as NaOAc and mixtures of toluene / methanol (5:1) as solvent may induce the formation of the *cis*- isomers of compounds [$PtCl_2$(N-donor ligand)(dmso)] or even cycloplatinated complexes [23b-e,47,48], we also investigated whether for ligand **1a** the addition of NaOAc could affect the nature of the final Pt(II) product. When equimolar amounts of **1a**, *cis*-[$PtCl_2(dmso)_2$] and NaOAc were refluxed in a mixture of toluene : methanol (5:1) for 72 h (Table 2, entry *VI* and Scheme 2), the ^{1}H-NMR spectrum of the raw material in $CDCl_3$ at 298 K (Fig. S4) revealed the coexistence of **3a** and a minor product (hereinafter referred to as **4a**). The work-up of a column chromatography allowed us to isolate complex **3a** and a solid containing a mixture of **3a** and **4a**. The $^{195}Pt\{^{1}H\}$ NMR spectrum of the solid dissolved in $CDCl_3$ at 298 K (Fig. S1, **A**) showed two singlets (one at δ = -2980 ppm (due to **3a**) and the other at δ = -2932 ppm assigned to compound **4a**). Their chemical shifts suggest that the environment of the Pt(II) atoms in **3a** and **4a** should be very similar. Moreover, the separation between the two singlets (ca. 41 ppm), falls in the typical range reported for *trans*- and *cis*- isomers of [Pt(N-donor)Cl_2(dmso)] compounds. Besides that, its ^{1}H-NMR spectrum (Fig. S1, **B**) revealed that for **4a** the resonances due to the protons of the dmso ligand appeared as two singlets, in good agreement with a *cis*- disposition of the Cl^- ligands. On these basis we assumed that **4a** is the *cis*- isomer of [$PtCl_2$(**1a**)(dmso)]. Unfortunately, attempts

to isolate **4a** in its pure form, by fractional crystallization or subsequent column chromatography failed.

Comparison of ^{1}H-NMR spectra of the new complexes (**2a**, **3a** and **4a**) with that of the parent ligand **1a** reveals that the resonances due to the H^2 and H^4 protons of the carbazole array were highly affected by the binding of the nitrogen to the Pt(II) ion. It should be noted that: a) the formation of the Pt-$N_{(thiazole)}$ bond requires the cleavage of the intramolecular C11-H12···N hydrogen bond, b) in *cis*- and *trans*- isomers of [$PtCl_2$(N-heterocycle)(dmso)] complexes, the heterocycle is orthogonal to the main coordination plane of the ligand [23d-e,49,50], and c) frequently ancillary ligands (Cl^- or dmso) are involved in additional C-H ···X [X = Cl or $O_{(dmso)}$] contacts with the neutral N-donor ligand [49,50]. All these findings could explain the variations observed in the chemical shifts of the protons adjacent to position 3 in complexes **3a** and **3b**.

In order to compare the potential coordination ability of the two new carbazoles, the reactivity of the thienyl derivative **1b** with [$MCl_2(dmso)_2$] and $Na_2[PdCl_4]$ was studied under identical conditions as for **1a** (described above and shown in Scheme 2) and using identical conditions as those shown in Table 2 (entries *I* - *IV*). However, none of these studies allowed us neither the isolation or even the detection by ^{1}H-NMR of any Pd(II) or Pt(II) complex, thus suggesting that thiazole-substituted carbazole **1a** has a greater coordination ability than the thienyl analogue **1b**.

3.2. Electronic spectra and optical properties

Absorption spectra of CH_2Cl_2 solutions of **1a** and **1b** at 298 K (Table 3 and Fig. S5, **A**) showed two intense bands in the range 250–450 nm that are characteristic of carbazoles. The corresponding UV-vis spectra of the complexes **2a** and **3a** (Fig. S5, **B** and Table 3) exhibited two intense absorption bands in the range $300 \leq \lambda < 350$ nm. One of them shifted to lower energies in relation to the free ligand being for the Pt(II) complex (**3a**) the magnitude of the shift bigger than for the Pd(II) complex **2a** (Table 3). These findings suggest that this absorption band is due to a metal perturbed intra-ligand electronic transition (MPILET). The second absorption band, at

higher energies, is practically coincident with that of the free ligand. The spectra of compounds **2a** and **3a** (Fig. S5, **B**) also exhibited an additional and poorly resolved absorption band at lower wavelengths [$280 \leq \lambda < 290$ nm].

Table 3. Absorption and emission properties of the free carbazoles (**1a** and **1b**) and the Pd(II) and Pt(II) complexes (**2a** and **3a**, respectively) in CH_2Cl_2 [Wavelengths λ_i (in nm), logarithms of the extinction coefficients (log ε_i), emission wavelengths [λ_{em} (in nm) after excitation at λ_{exc} = 300 nm] and quantum yields (Φ).

	Absorption spectroscopic data	**Emission spectroscopic data**	
Compd.	**λ (log ε)**	**λ_{em}**	**Φ**
1a	328 (4.3), 301 (4.5), 279 sh (≈ 4.2)	370 sh, 384	0.22
1b	317 (≈ 4.2), 299 (4.5)	376, 394	0.12
2a	334 (3.6), 300 (3.8), 284 (≈ 3.8)	370 sh, 385	0.02
3a	345 (4.2), 301 (4.4), 287 (4.4)	370 sh, 386	< 0.01

The emission spectra of **1a**, **1b**, **2a** and **3a** were recorded in CH_2Cl_2 solution at 298 K. Upon excitation at λ_{exc} = 300 nm, the free ligands **1a** and **1b** exhibited emission bands in the range 370-395 nm (Fig. S6 and Table 3). The thienyl-based derivative **1b** showed a bathochromic shift of the wavelength of maximum emission of 10 nm in comparison to the thiazolyl-based ligand **1a**, according to the strongest electron-donating character of the thienyl unit. It should be noted that the quantum yield of **1a** (Table 3) is significantly higher than that of **1b**. Complexes **2a** and **3a** exhibited also emission bands consistent with that of ligand **1a**, but their fluorescence quantum yields [51] decreased considerably in relation to the free ligand (**1a**).

3.3. Computational studies

In order to elucidate the effect produced by the thiazolyl or thienyl groups of compounds **1a** and **1b** on the electronic delocalization, computational calculations based on the DFT methodology were undertaken [31]. Calculations were carried out using the B3LYP hybrid functional [32,33] and the 6-31G* basis set [35] implemented in the Gaussian03 program [34]. In a first stage, geometries of compounds **1a** and **1b** were optimized without imposing any

restriction. Final atomic coordinates for the optimized geometries are included as supplementary information (Tables S1-S2). Bond lengths and angles of the optimised geometry of **1a** were consistent with those obtained from the X-ray studies (the differences did not clearly exceed 3σ) and those of **1b** are in the range reported for related carbazoles with mono or polythienyl units on position 3 [20,50].

Molecular orbital (MO) calculations of the optimized geometries revealed that highest occupied molecular orbital (HOMO) (Fig. 4) of **1a** and **1b** are very similar except for a tiny difference in the contribution of the atomic orbitals of the sulphur atom. The LUMO (Fig. 4) of **1a** is mainly centred on the thiazolyl unit and two of the rings of the carbazole; while in **1b**, the contribution of the thienyl decreases in relation to that of the thiazole in **1a**. Moreover, the HOMO-LUMO gap (ΔE) of **1b** (4.32 eV) is higher than for **1a** (4.14 eV). These findings suggest that the replacement of the thiazolyl ring of **1a** by the thienyl in **1b** reduces the electronic delocalization mentioned above.

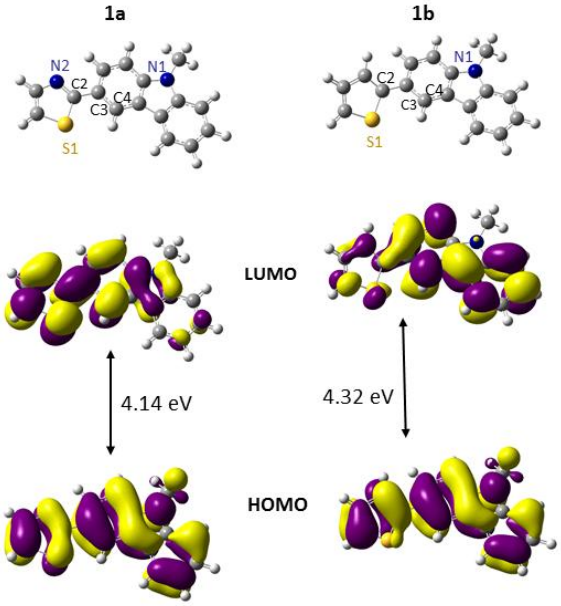

Fig. 4. Highest occupied molecular orbital (HOMO) and lowest unoccupied molecular orbital (LUMO) for the new carbazole derivatives (**1a** and **1b**).

In the optimized geometry of **1b** the intramolecular separation between the S1 atom and the hydrogen atom of phenyl ring (2.848 Å) is larger than in **1a** [S1···H: 2.748 Å (optimized

geometry) or 2.751 Å (from the crystal structure)] and the angle formed by the heterocycle and the carbazole is 30.3° bigger than in **1a**. Since it is well-known that deviations from planarity affects the electronic delocalization, the properties of the compounds and their potential utility, we also calculated the energy of the molecules for different orientations of the attached heterocycle versus the carbazole unit using molecular mechanics. These arrangements were generated by modifying the torsion angle defined by the set of atoms S1-C2'-C3-C4 (hereinafter referred to as φ) from 0° to 360°. The results shown in Fig. 5, reveal that for **1a** the minimum energy corresponds to φ values in the ranges (0° ≤ φ ≤ 16° and 344°≤ φ ≤ 360°), that is to say close to co-planarity, similar to that found in the crystal structure φ = 13.5° and with the S1 atom and NMe group located in opposite sides.

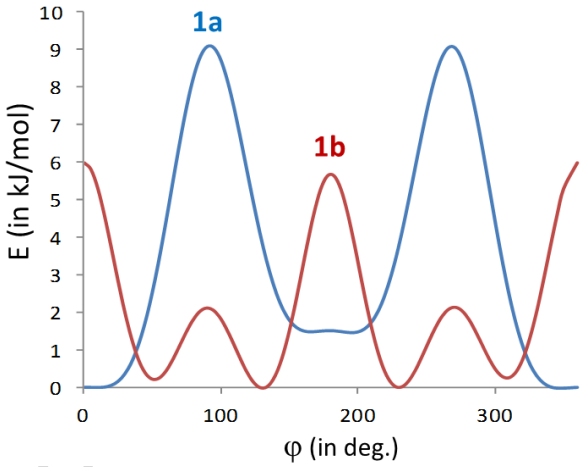

Fig. 5. Plot of the energy of the molecule of **1a** (blue) or **1b** (red) versus the value of the torsion angle S1-C2'-C3-C4 (φ).

The energy barrier to achieve an orthogonal arrangement of the thiazole (φ = 90° or 270°) is rather high (9.1 kJ/mol). The conformer with the N1 and N2 atoms on opposite sides, [φ values between 164° and 196°] is slightly less stable than for φ = 0 ± 16 ° (Fig. 5). The differences between the energies of both conformers determined from molecular mechanics calculations and DFT are 0.4 and 0.5 Kcal/mol, respectively.

In contrast with the results obtained for **1a**, in **1b** the most favourable orientation of the thienyl unit is far away from co-planarity and corresponds to φ values in the ranges 128° - 133°

and 232° - 237°. The energy barriers to achieve coplanar arrangements (Fig. 5) are smaller than that obtained for **1a** (9.1 kJ/mol); consequently, from an energetic point of view, the free rotation of the thienyl unit, that requires a smaller energy income, is more likely to occur than that of the thiazolyl ring of **1a**. In addition, time dependent DFT (TD-DFT) calculations were performed to achieve the assignment of the bans observed in the UV-vis spectra (Table S4 and Fig. S7).

3.4. Biological studies

3.4.1. Antiproliferative assay

We have evaluated the cytotoxic activity of ligands **1a** and **1b** and the new complexes **2a** and **3a** in front of the colon cell line HCT116 and two breast cancer cell lines [the triple negative (ER, PR and no HER2 over expression) MDA-MB231 and the MCF7]. The effects of the new products on the growth of the three cell lines and that of cisplatin, used as positive control, were assessed after 72 h and the results are presented in Table 4 and Fig. 6.

The comparison of the *in vitro* cytotoxic activities of the free carbazoles **1a** and **1b** in the HCT116 cell line revealed that the replacement of the thienyl ring (in **1b**) by the thiazolyl unit of **1a** produced a significant enhancement of the cytotoxic potency. This trend is practically identical to those observed in the two breast (MDA-MB231 and the MCF7) cancer cell lines and could be attributed to several factors. One of these could be the lipophilicity that, as shown in Table 4, is expected to be slightly different for the two systems. It should be noted that in the MCF7 cell line ligand **1a** is (ca. 9.5 times) more potent than cisplatin, the non-alkylated 9*H*-carbazole (IC_{50} > 40 μM) and even than doxorubicin (IC_{50} = 7.3 μM).

Table 4. Cytotoxic activities (IC_{50} values[a], μM) on HCT-116 (colon), MDA-MB-231 and MCF7 (breast) cell lines, for the palladium(II) and platinum(II) complexes derived from **1a** (**2a** and **3a**, respectively) and for cisplatin. For comparison purposes, *Clog P* values[b] and lipophilic efficiencies (*LipE*[c]) of compounds **1a**, **1b**, **2a** and **3a** on the MCF7 cell line are also included (nd = not determined).

Compounds	IC_{50} values in the cancer cell lines [a]			*ClogP* [b]	*LipE* [c]
	HCT116	MDA-MB231	MCF7		
Carbazoles					
1a	31 ± 2	9.4 ± 2.6	2.0 ± 0.5	4.42	1.27
1b	50 ± nd	51 ± nd	47 ± nd	5.73	-1.39
Complexes					
2a	> 100	> 100	24 ± 2	9.42	-4.80
3a	34 ± nd	37 ± nd	2.4 ± 2.2	4.33	1.29
Cisplatin	40 ± 4.4	6.5 ± 2.4	19 ± 4.5	-------	-------

[a] Data are shown as the mean values of two experiments performed in triplicate. [b] *ClogP* is the calculated logarithmic value of the n-octanol/water partition coefficient and was calculated using the ChemBioDrawUltra computer program. [c] *LipE* indexes were calculated as *LipE* = - log(IC_{50})- *ClogP* [52] and using the IC_{50} values obtained in the MCF7 cell line.

In order to compare the effect produced by the binding of the Pd(II) or Pt(II) we also examined the effect produced by the complexes **2a** and **3a** on identical cell lines. As shown in Table 4 and Fig. 6, the Pd(II) complex **2a** did not show any relevant antiproliferative activity (IC_{50} > 100 μM) in the HCT116 and MDA-MB213 cell lines. In the MCF7 it was more active, but its potency was slightly smaller (IC_{50} = 24 ± 2.2 μM) than that of the reference cisplatin (IC_{50} = 19 ± 4.5 μM). In contrast, the Pt(II) complex (**3a**) exhibited a higher inhibitory growth effect, being 9 times more potent than the reference drug in the MCF7 breast cancer cell line.

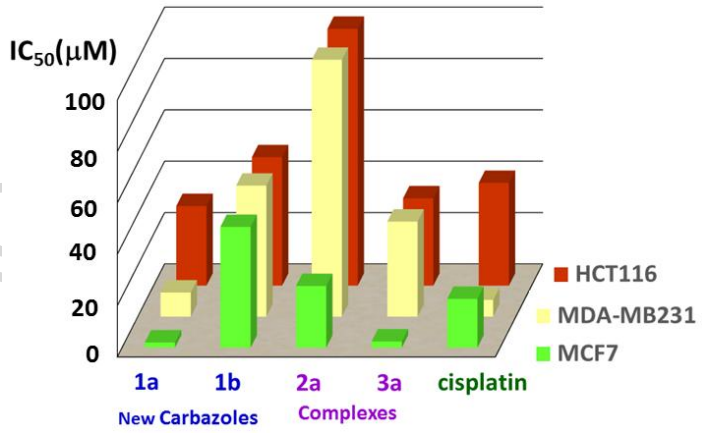

Fig. 6. Comparative plot of the IC_{50} values (in μM) of the new carbazoles (**1a** and **1b**), the Pd(II) and Pt(II) complexes derived from **1a** and cisplatin in front of the colon cancer cell line (HCT116) and the two breast cancer cell lines (MDA-MB231 and MCF7).

It is well-known that the preparation of new products with improved cytotoxic potency is not the unique requirement in medicinal chemistry and drug design, other factors such as the lipophilicity that contributes to the ADMET (absorption, distribution, metabolism excretion and toxicity) properties of drugs also plays a crucial role. Nowadays, the lipophilic efficiency (*LipE*) index [52] that includes lipophilicity and potency is becoming more and more popular in drug design and optimization, because it allows to normalize the observed potency with changes in the lipophilicity.

In view of this, we calculated the clog values for the new compounds and their *LipE* index in the MCF7 cell line. The results (Table 4) reveal that for the compounds characterized in this work the *LipE* index increases as follow **2a** << **1b** < **1a** ≤ **3a**. The Pd(II) complex **2a** that shows low solubility it is simultaneously the most lipophilic and the less potent compound of the series. In contrast with these results, for the carbazole-thiazole ligand **1a** and its *trans*-[$PtCl_2$(**1a**)(dmso)] complex **3a** there is an effective combination of their cytotoxic potency in MCF7 and lipophilicity, and on these basis they are promising scaffolds in the search of optimized drugs. Chemical modifications of the core of ligand **1a**, its binding to the Pt(II) atom or even changes on the ancillary ligands bound to it in **3a** may allow to tune the lipophilicity and to improve the lipophilic efficiency.

3.4.2. Additional studies to elucidate the mechanism of action

In the majority of the described cases of cytotoxic carbazoles, they act as DNA-intercalators or as Topoisomerase I/II (or telomerases) inhibitors [53], although other mechanisms of action involving different targets {i.e. estrogen receptors (ER) or cyclin dependent kinases (CDK), among others} have also been postulated [10,11,54]. To examine whether the presence of the thiazole (in **1a**) or the thienyl unit (in **1b**) in the free ligand and the binding of **1a** to the Pd(II) or Pt(II) ions in complexes **2a** and **3a**, could have an important role in the mechanism of action, additional experiments were performed.

To elucidate whether compounds **1a**, **1b**, **2a** and **3a** act as DNA intercalators or as Topoisomerase I or II inhibitors, three different sets of experiments were undertaken. In a first

stage it was examined if the new compounds could induce changes in the electrophoretic mobility of the supercoiled closed form (ccc) of pBluescript SK^+ plasmid DNA. For DNA migration studies, the plasmid was incubated with compounds **1a, 1b, 2a** and **3a** at increasing concentrations ranging from 0 μM to 200 μM. For comparison purposes, incubation of DNA with cisplatin (CDDP) or ethidium bromide (EB) was also performed. As expected, cisplatin greatly altered the electrophoretic mobility of pBluescript DNA at all concentrations tested. As depicted in Fig. 7, the free ligands (**1a** and **1b**) and the Pd(II) compound (**2a**) were not effective. Only the Pt(II) complex (**3a**) produced a significant effect on the electrophoretic mobility of native pBluescript DNA at concentrations greater than 100 μM.

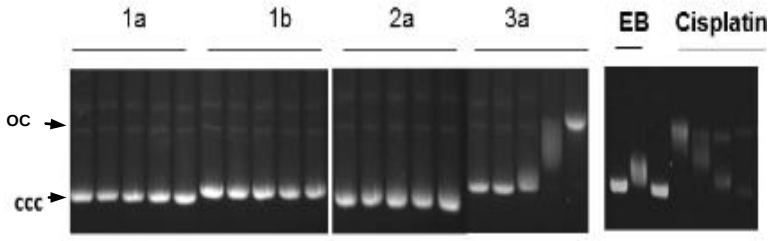

Fig. 7. Interaction of pBluescript SK^+ plasmid DNA (40 μg/ml) with increasing concentrations of compounds **1a**, **1b**, **2a** and **3a**, ethidium bromide (EB) and cisplatin. Lane 1: DNA only; Lane 2: 1 μM; Lane 3: 2.5 μM; Lane 4: 5 μM and Lane 5: 10 μM; Lane 6: 25 μM; Lane 7: 50 μM; Lane 8: 100 μM; Lane 9: 200 μM. ccc represents the supercoiled closed circular form and oc the open circular form.

Secondly, a Topoisomerase based gel assay was performed to evaluate the ability of compounds **1a**, **1b** and **2a** to intercalate into DNA or to act as DNA Topoisomerase I inhibitors. For that, supercoiled pBluescript plasmid DNA was incubated with Topoisomerase I in the presence of increasing concentrations of the compounds under study. The results are presented in Fig. 8, where ethidium bromide (EB) was used as an intercalator control. The analysed compounds did not prevent unwinding of DNA indicating that they are neither intercalators nor Topoisomerase I inhibitors.

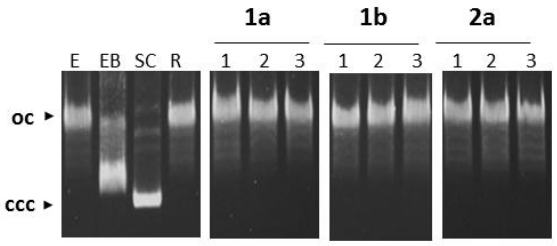

Fig. 8. Analysis of the new ligands (**1a** and **1b**) and compound **2a** as potential DNA intercalators or Topoisomerase I inhibitors. Conversion of supercoiled pBluescript SK+ DNA (40 μg/mL) to relaxed DNA by the action of Topoisomerase I (3 units) in the absence or in the presence of increasing amounts of compounds. **E** = 100 μM etoposide; **EB** = 10 μM Ethidium Bromide; **SC** = supercoiled DNA as control; **R** = relaxed DNA by the action of Topoisomerase I as control; Lane 1: 25 μM; Lane 2: 100 μM; Lane 3: 200 μM; ccc= closed circular form and oc = open circular form.

As mentioned above, another important target for antitumor agents is the Topoisomerase II, which is associated with solving the topological constraints of DNA by transiently cleaving both strands of the double helix [53]. In humans there are two Topoisomerase II isoenzymes, IIα and IIβ. Here we study the capability of compounds **1a**, **1b** and **2a** as catalytic inhibitors of Topoisomerase IIα. The inhibitory activity was evaluated by measuring the extent of enzyme mediated relaxed DNA after treatment with 200 μM of **1a**, **1b** or **2a** compounds. Only the Pd(II) complex **2a** showed at this concentration inhibitory activity (Fig. 9).

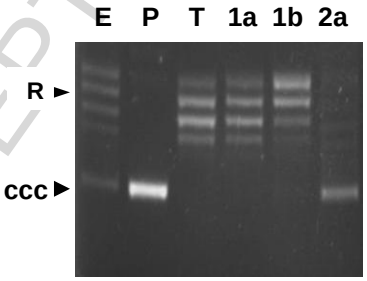

Fig 9. Topoisomerase-II α inhibitory activity of compounds **1a**, **1b** and **2a**. Reactions contained supercoiled plasmid DNA, Topoisomerase IIα (4 units) and 200 μM of the indicated compound. Control reactions were performed in the presence of: **E**, etoposide at 100 μM; **P**: SC Plasmid DNA only; **T**: reaction performed with plasmid DNA and Topoisomerase IIα (4 units).

Other mechanism of action implies Cathepsin B, which is a cysteine metaloprotease that could be involved in metastasis, angiogenesis and tumour progression. Examples of Pd(II) and

Pt(II) complexes as inhibitors of Cathepsin B have been reported [55]. However, none of the new compounds presented in this work (**1a**, **1b** and **2a**) inhibited the enzyme activity at 100 μM concentration.

Overall the biological studies undertaken with the new compounds **1a**, **1b**, **2a** and **3a** provide conclusive evidences. The DNA migration studies revealed that only Pt(II) complex (**3a**) modifies the electrophoretic mobility of the plasmid in a similar way as cisplatin but at higher concentrations. Experimental results also revealed that neither compounds **1a**, with higher cytotoxic activity than cisplatin in the tested cancer lines HCT116 and MCF7, nor compounds **1b** or **2a** operate as intercalators or as inhibitors of cathepsin B or Topoisomerase I. However, the Pd(II) complex (**2a**) inhibits the activity of Topoisomerase IIα (at 200 μM concentration).

As a summary, among the new compounds, **1a** and its Pt(II) complex are the most active in the assayed HCT116, MDA-MB231 and MCF7 cancer cell lines. Moreover, compound **1a**, clearly more potent than **3a**, has an additional interest due to its low toxiticy on the normal and non-tumoral human skin fibroblast BJ cell line (IC_{50} > 100 μM for **1a** versus IC_{50} = 23 ± 2 μM for cisplatin under identical experimental conditions). This finding enhances the interest and relevance of carbazole **1a** for further and additional biological studies.

4. Conclusions

Here we have presented two new *N*-methylated and 3-substituted carbazoles with a thiazolyl (**1a**) or a thienyl (**1b**) unit and comparative studies of their properties and reactivity in front of $Na_2[PdCl_4]$ or $[MCl_2(dmso)_2]$ (M = Pd or Pt) and biological activities. The obtained results proved that compound **1a** is clearly more reactive than **1b** and has a greater coordination capability towards the Pd(II) and Pt(II) ions, leading to *trans*-$[PdCl_2(\mathbf{1a})_2]$ (**2a**) and the geometrical isomers {*trans*- (**3a**) or *cis*- (**4a**)} of $[PtCl_2(\mathbf{1a})(dmso)]$. Computational studies have allowed us to explain the effect produced by the thiazolyl and thienyl units on: a) their relative orientation in relation to the backbone of the carbazole, b) the electronic delocalization, c) the distribution of charge and d) the origin of the bands observed in their absorption spectra and their assignment.

The results obtained from *in vitro* studies on the cytotoxic activity of compounds **1a**, **1b**, **2a** and **3a** in the HCT116, MDA-MB231 and MCF7 cancer cell lines show that: a) the replacement of the thiazole (of **1a**) by the thienyl (to give **1b**) reduces the inhibitory growth effect, b) the binding of **1a** to the Pt(II) atom (**3a**) reduces its cytotoxic activity and c) compound **2a**, with two units of **1a**, bound to the Pd(II) is less active than the Pt(II) complex **3a** and only showed moderate activity in the MCF7 cell line. Additional biological studies aimed to clarify the mechanism of action of the new compounds revealed that: a) only the Pt(II) complex (**3a**) induced significant changes on the electrophoretic mobility of the pBluescript DNA, but at higher concentrations than the cisplatin and b) neither the ligands (**1a** and **1b**) nor the Pd(II) complex (**2a**) acted as intercalators or inhibitors of Topoisomerase I or Cathepsin B. However, the Pd(II) complex (**2a**) with an inhibitory growth activity in the MCF7 cell line (IC_{50} = 24 $\pm$ 2 μM) similar to that of cisplatin (IC_{50} 19 $\pm$ 4.5 μM) inhibited the Topoisomerase IIα activity. These findings suggest that the binding of the Pd(II) or the Pt(II) to the carbazole **1a** not only produces significant changes in their cytotoxic activity but also on their mechanism of action.

Among the new compounds presented here, carbazole **1a**, appears to be particularly attractive because: a) it is clearly more cytotoxic than **1b** in the three cancer cell lines used in this study; b) its inhibitory growth effect is quite similar (in MDA-MB231 and in the cisplatin resistant HCT116 cell line) or ca. 9-times greater than *cisplatin* in the MCF7 cell line and c) it does not contain Pt(II) and consequently might not produce the typical and undesirable side effects of conventional Pt(II)-based drugs. These findings together with: a) its high stability in the solid state and also in dmso (Fig. S9) or in mixtures dmso: D_2O (Fig. S10-S12) at 298 K and b) its photo-physical properties make of compound **1a** an excellent candidate for further studies in order to elucidate its effect on a wider panel of cancer cell lines, its mechanism of action, in combined therapies even in photodynamic therapy, and to explore other biological activities (i.e. antibacterial, antifungal, etc.) that are relevant in new drug design and development.

Acknowledgements

This work was supported by the *Ministerio de Ciencia e Innovación* of Spain (MICINN) (Grant numbers CTQ2015-65040-P and CTQ2015-65770-P MINECO/FEDER).

Appendix A. Supplementary material

Tables containing: final atomic coordinates of the optimised geometries of carbazoles **1a** and **1b** (Tables S1 and S2, respectively), calculated energies of the HOMO and LUMO orbitals, energy gaps ($\Delta E = E_{LUMO} - E_{HOMO}$) for the new carbazoles and calculated values of the Mulliken charges of selected atoms (Table S3), summary of the results obtained from the computational studies showing electronic transitions with greater contributions in the absorption bands for **1a** and **1b** (Table S4) and additional Figures (Figs. S1-S12) showing: the ^{1}H-NMR spectrum of compound **3a** (Fig. S2); an expansion of the ^{1}H-NMR spectrum of the raw material obtained after 24 h under reflux, showing the presence of complex **3a** and another minor product (Fig. S3); the ^{1}H-NMR spectrum of the crude material obtained after 72 h that shows the coexistence of **3a** and an additional product **4a** (Fig. S4); The ^{195}Pt{^{1}H} and ^{1}H-NMR spectra of the mixture of the two isomers of [$PtCl_2$(**1a**)(dmso)] {*trans*- (**3a**) and *cis*- (**4a**)}, isolated from the column (Fig. S1); UV-Vis spectra of compounds **1a**, **1b**, **2a** and **3a** (Fig. S5), emission spectra of compounds **1a**, **1b**, **2a** and **3a** (Fig. S6); calculated absorption spectra of compounds **1a** and **1b** (Fig. S7); the HOMO-1 and LUMO+1 orbitals for carbazoles **1a** and **1b** (Fig. S8); and Figures (Fig. S9-S12); showing the ^{1}H-NMR spectra of a freshly prepared solution of compound **1a** in dmso-d_6 (Fig. S9) or in mixtures dmso-d_6: D_2O (from 4:1 to 1:1) (Fig. S10-S12) after several periods of storage at 298 K.

Notes and references

[1] Cancer Facts & Figures 2017, American Cancer Society. http://www.cancer.org/research/cancerfactsstatistics/cancerfactsfigures2017/index, 2017 (accessed May 2017).

[2] Cancer statistics center, American Cancer Society. https://cancerstatisticscenter.cancer.org/?_ga=1.48498790.1307978637.1460725255#/, 2017 (accessed May 2017).

[3] A.B. Ryerson, C.R. Eheman, S.F. Altekruse, J.W. Ward, A. Jemal, R.L. Sherman, S.J. Henley, D. Holtzman, A. Lake, A.-M. Noone, R.N. Anderson, J. Ma, K.N. Ly, K.A. Cronin, L. Penberthy, B.A. Kohler, Annual Report to the Nation on the Status of Cancer, 1975-2012, Featuring the Increasing Incidence of Liver Cancer, Cancer 122 (2016) 1312-1337.

[4] Updated information on colorectal and breast cancer can be obtained from the American Cancer Society, Atlanta, Georgia, USA (http://www.cancer.org/acs) through a) www.cancer.org/acs/groups/content/documents/document/acspc-042280.pdf and b) www.cancer.org/acs/groups/content/documents/document/acspc-04638.pdf (for colorectal cancer and breast cancer, respectively) (accessed May 2017).

[5] G.F. Weber, Molecular Therapies of Cancer, Springer, Germany, 2015.

[6] a) A.C. Flick, H.X. Ding, C.A. Leverett, R.E. Kyne Jr., K.K.-C. Liu, S.J. Fink, C.J. O'Donnell, Synthetic approaches to the 2014 new drugs, Bioorg. Med. Chem. 24 (2016) 1937-1980; b) N.A. Meanwell, Improving Drug Design: An Update on Recent Applications of Efficiency Metrics, Strategies for Replacing Problematic Elements, and Compounds in Nontraditional Drug Space, Chem. Res. Toxicol. 29 (2016) 564-616; c) A.L. Harvey, R.L. Clark, S.P. Mackay, B.F. Johnston, Current strategies for drug discovery through natural products, Expert Opin. Drug Discovery 5 (2010) 559-568; d) E.A.G. Blomme, Y. Will, Toxicology Strategies for Drug Discovery: Present and Future, Chem. Res. Toxicol. 29 (2016) 473-504; e) S.A. McKie, Polypharmacology: *in silico* methods of ligand design and development, Future Med. Chem. 8 (2016) 579-602; f) I. Ali, M.N. Lone, Z.A. Al-Othman, A. Al-Warthan and M.M. Sanagi, Heterocyclic Scaffolds: Centrality in Anticancer Drug Development, Curr. Drug Targets 16 (2015) 711-734.

[7] a) Comprehensive Heterocyclic Chemistry III, A.R. Katritzky, C.A. Ramsden, E.F.V. Scriven, R.J.K. Taylor (Eds.), Elsevier, Oxford (UK), 2008; b) R.K. Parashar, Chemistry of Heterocyclic Compounds, CRC Press, 2014; c) A.F. Pozharskii, A.T. Soldatenkov, A.R. Katritzky, Heterocycles in Life and Society: An Introduction to Heterocyclic Chemistry, Biochemistry and Applications, second ed., Wiley-VCH, Weinheim (Germany), 2011.

[8] a) Comprehensive Coordination Chemistry II: From Biology to Nanotechnology; J.A. McCleverty, T.J. Meyer (Eds.), Elsevier, Amsterdam, 2003; b) Comprehensive Organometallic Chemistry III, R.H. Crabtree, D.M.P. Mingos (Eds.), second ed., Elsevier, Oxford, UK, 2007; c) Comprehensive Coordination Chemistry: The Synthesis, Reactions, Properties and Applications of Coordination Compounds, G. Wilkinson, R.D. Gillard, J.A. McCleverty (Eds.), Pergamon Press: Oxford, UK, 1987.

[9] a) J.J. Li, Heterocyclic Chemistry in Drug Discovery, John Wiley & Sons, Hoboken, USA, 2013; b) T.Y. Zhang, Chapter One - The Evolving Landscape of Heterocycles in Drugs and Drug Candidates, E.F.V. Scriven, C.A. Ramsden (Eds.), In Advances in Heterocyclic Chemistry, Academic Press, 121 (2017) 1-12; c) A. Gomtsyan, Heterocycles in drugs and drug discovery, Chem. Heterocycl. Compd. 48 (2012) 7-10; d) P. Martins, J. Jesús, S. Santos, L.R. Raposo, C. Roma-Rodrigues, P.V. Baptista, A.R. Fernandes, Heterocyclic Anticancer Compounds: Recent Advances and the Paradigm Shift towards the Use of Nanomedicine's Tool Box, Molecules 20 (2015) 16852-16891.

[10] For a recent review on carbazole derivatives in medicinal and natural products see: L.S. Tsutsumi, D. Gündisch, D. Sun, Carbazole Scaffold in Medicinal Chemistry and Natural Products: A Review from 2010-2015, Curr. Top. Med. Chem. 16 (2016) 1290-1313.

[11] a) K.N. Mounika, A.N. Jyothy, G.N. Raju, R.R. Nadendla, Carbazole derivatives in cancer treatment - a review, World J. Pharm. Pharm. Sci. 4 (2015) 420-428; b) M. Bashir, A. Bano, A.S. Ijaz, B.A. Chaudhary, Recent Developments and Biological Activities of *N*-Substituted Carbazole Derivatives: A Review, Molecules 20 (2015) 13496-13517; c) C. Asche, M. Demeunynck, Antitumor Carbazoles, Anti-Cancer Agents Med. Chem. 7 (2007) 247-267; d) A. Caruso, D. Iacopetta, F. Puoci, A.R. Cappello, C. Saturnino, M.S. Sinicropi, Carbazole derivatives: a promising scenario for breast cancer treatment, Mini-Rev. Med. Chem. 16 (2016) 630-643.

[12] For a general overview of recent advances in thiazoles as antitumor agents: a) J. Paneer-Selvam, G. Saravanan, M. Palenivelu, Anticancer Evaluation of Thiazole Based Heterocycles - A Review, Lambert Academic Publishing, Saarbrücken, Germany, 2014; b) A. Ayati, S. Emami, A. Asadipour, A. Shafiee, A. Foroumadi, Recent applications of 1,3-thiazole core structure in the identification of new lead compounds and drug discovery, Eur. J. Med. Chem. 97 (2015) 699-718; c) A. Chawla, H. Kaur, P. Chawla, U.S. Baghel, A review on chemistry and biological activities of thiazole derivatives, J. Global Trends Pharm. Sci. 5 (2014) 1641-1648; d) A. Leoni, A. Locatelli, R. Morigi, M. Rambaldi, Novel thiazole derivatives: a patent review (2008 - 2012; Part 1), Expert Opin. Ther. Patents 24 (2014) 201-216.

[13] For articles on the uses of thiophene derivatives as antitumor drugs: a) K.K. Jha, S. Kumar, I. Tomer, R. Mishra, Thiophene: the molecule of diverse medicinal importance, J. Pharm. Res. 5 (2012) 560-566; b) M.M. Ghorab, M. S. Bashandy, M.S. Alsaid, Novel thiophene derivatives with sulfonamide, isoxazole, benzothiazole, quinoline and anthracene moieties as potential anticancer agents, Acta Pharm. 64 (2014) 419-431; c) D. Gramec, L.P. Mašič, M.S. Dolenc, Bioactivation Potential of Thiophene-Containing Drugs, Chem. Res. Toxicol. 27 (2014) 1344-1358.

[14] a) N.C. Garbett, D.E. Graves, Extending Natures Leads: The Anticancer Agent Ellipticine, Curr. Med. Chem.: Anti-Cancer Agents 4 (2004) 149-172; b) C.M. Miller, F.O. McCarthy, Isolation, biological activity and synthesis of the natural product ellipticine and related pyridocarbazoles, RSC Adv. 2 (2012) 8883-8918.

[15] a) R.K. Mehmood, Review of Cisplatin and Oxaliplatin in Current Immunogenic and Monoclonal Antibody Treatments, Oncol. Rev. 8 (2014) 256; b) F.M. Muggia, A. Bonetti, J.D. Hoeschele, M. Rozencweig, S.B. Howell, Platinum Antitumor Complexes: 50 Years Since Barnett Rosenberg's Discovery, J. Clin. Oncol. 33 (2015) 4219-4226; c) S. Amptoulach, N. Tsavaris, Neurotoxicity Caused by the Treatment with Platinum Analogues, Chemother. Res. Pract. (2011) (art. ID. 843019) [http: //dx.doi.org/10.1155/2011/843019].

[16] a) M.A. Jordan, Mechanism of Action of Antitumor Drugs that Interact with Microtubules and Tubulin, Curr. Med. Chem.: Anti-Cancer Agents 2 (2002) 1-17; b) K. Chatterjee, J. Zhang, N. Honbo, J.S. Karliner, Doxorubicin Cardiomyopathy, Cardiology 115 (2010) 155-162.

[17] H. Jiang, J. Sun, J. Zhang, A Review on Synthesis of Carbazole-based Chromophores as Organic Light-Emitting Materials, Curr. Org. Chem. 16 (2012) 2014-2025.

[18] a) M. Reig, G. Bagdziunas, D. Volyniuk, J.V. Grazulevicius, D. Velasco, Tuning the ambipolar charge transport properties of tricyanovinyl-substituted carbazole-based materials, Phys. Chem. Chem. Phys. 19 (2017) 6721-6730; b) M. Reig, C. Gozálvez, R. Bujaldón, G. Bagdziunas, K. Ivaniuk, N. Kostiv, D. Volyniuk, J.V. Grazulevicius, D. Velasco, Easy accessible blue luminescent carbazole-based materials for organic light-emitting diodes, Dyes Pigm. 137 (2017) 24-35; c) M. Reig, G. Bubniene, W. Cambarau, V. Jankauskas, V. Getautis, E. Palomares, E. Martínez-Ferrero and D. Velasco, New solution-processable carbazole derivatives as deep blue emitters for organic light-emitting diodes, RSC Adv. 6 (2016) 9247-9253; d) M. Reig, J. Puigdollers, D. Velasco, Molecular order of air-stable p-type organic thin-film transistors by tuning the extension of the π-conjugated core: the cases of indolo[3,2-*b*]carbazole and triindole semiconductors, J. Mater. Chem. C 3 (2015) 506-513; e) J. L. Díaz, A. Dobarro, B. Villacampa, D. Velasco, Structure and Optical Properties of 2,3,7,9-Polysubstituted Carbazole Derivatives. Experimental and Theoretical studies, Chem. Mater. 13 (2001) 2528-2536.

[19] a) B.-B. Ma, Y.-X. Peng, T. Tao, W. Huang, A distinguishable photovoltaic performance on dye-sensitized solar cells using ruthenium sensitizers with a pair of isomeric ancillary ligands, Dalton Trans. 43 (2014) 16601-16604; b) Y.-X. Li, X.-T. Tao, F.-J. Wang, T. He, M.-H. Jiang, Structurally tailored thiophene-based hybrid materials for thin-film and single-

crystal transistors: Synthesis, photophysics and carrier-transport properties, Org. Electron. 10 (2009) 910-917.

[20] a) S.-I. Kato, S. Shimizu, A. Kobayashi, T. Yoshihara, S. Tobita, Y. Nakamura, Systematic Structure-Property Investigations on a Series of Alternating Carbazole-Thiophene Oligomers, J. Org. Chem. 79 (2014) 618-629; b) S.-I. Kato, S. Shimizu, H. Taguchi, A. Kobayashi, S. Tobita, Y. Nakamura, Synthesis and Electronic, Photophysical, and Electrochemical Properties of a Series of Thienylcarbazoles, J. Org. Chem. 77 (2012) 3222-3232; c) P. Wang, Y. Ju, S.Y. Tang J.Y. Wu, H.P. Zhou, 9-Ethyl-3,6-bis(2-thienyl)carbazole, Acta Cryst., Sect. E, 63 (2007) o3671.

[21] a) M.A.T. Nguyen, A.K. Mungara, J.-A. Kim, K.D. Lee, S. Park, Synthesis, Anticancer and Antioxidant Activity of Novel Carbazole-based Thiazole Derivatives, Phosphorus, Sulfur Silicon Relat. Elem. 190 (2015) 191-199; b) M.S. Shaikh, M.B. Palkar, H.M. Patel, R.A. Rane, W.S. Alwan, M.M. Shaikh, I.M. Shaikh, G.A. Hampannavar, R. Karpoormath, Design and synthesis of novel carbazolo–thiazoles as potential anti-mycobacterial agents using a molecular hybridization approach, RSC Adv. 4 (2014) 62308-62320.

[22] Photodynamic Therapy from Theory to Applications, M.H. Adbel-Kader (Ed.), Springer, Heildelberg, Germany, 2014.

[23] Selected articles to illustrate the changes produced by the binding of Pd(II) or Pt(II) ions to heterocyclic compounds on their properties and activities see for instance: a) J.U. Chukwu, C. López, A. González, M. Font-Bardía, M.T. Calvet, R. Messeguer, C. Calvis, Pd(II) complexes with N-substituted pyrazoles as ligands. The influence of the R group [OMe *versus* NMe_2] of [1-{R–$(CH_2)_2$–}-3,5-Ph_2–(C_3HN_2)] on their cytotoxic activity on breast cancer cell lines, J. Organomet. Chem. 766 (2014) 13-21; b) E. Guillén, A. González, C. López, P.K. Basu, A. Ghosh, M. Font-Bardía, C. Calvis, R. Messeguer, Heterodi- (Fe, Pd/Pt) and Heterotrimetallic (Fe_2, Pd) Complexes Derived from 4-(Ferrocenylmethyl)-*N*-(2-methoxyethyl)-3,5-diphenylpyrazole as Potential Antitumoral Agents, Eur. J. Inorg. Chem. (2015) 3781-3790; c) A. González, J. Granell, C. López, R. Bosque, L. Rodríguez, M. Font-Bardía, T. Calvet, X. Solans, Hemilabile and luminescent palladium(II) azo-2-phenylindole complexes, J. Organomet. Chem. 726 (2013) 21-31; d) M. Tomé, C. López, A. Gonzalez, B. Ozay, J. Quirante, M. Font-Bardía , T. Calvet, C. Calvis, R. Messeguer, L. Baldomà and J. Badia, *Trans*- and *cis*-2-phenylindole platinum(II) complexes as cytotoxic agents against human breast adenocarcinoma cell lines, J. Mol. Struct. 1048 (2013) 88-97; e) C. López, A. González, R. Bosque, P.K. Basu, M. Font-Bardía, T. Calvet, Platinum(II) and palladium(II) complexes derived from 1-ferrocenylmethyl-3,5-diphenylpyrazole. Coordination, cyclometallation or transannulation?, RSC Adv. 2 (2012) 1986-2002.

[24] Z. Szafran, R.M. Pike, M.M. Singh, Microscale Inorganic Chemistry. A Comprehensive Laboratory Experience, John Wiley & Sons, New York, USA, 1991, 218.

[25] J.H. Price, A.N. Williamson, R.F. Schramm, B.B. Wayland, Palladium(II) and Platinum(II) Alkyl Sulfoxide Complexes. Examples of Sulfur-Bonded, Mixed Sulfur- and Oxygen-Bonded, and Totally Oxygen-Bonded Complexes, Inorg. Chem. 11 (1972) 1280-1284.

[26] S.H. Tucker, Iodination in the Carbazole Series, J. Chem. Soc. 129 (1926) 546-553.

[27] D.D. Perrin, W.L.F. Armarego, Purification of Laboratory Chemicals, fourth ed., Butterworth–Heinemann, Oxford, UK, 1996.

[28] G.M. Sheldrick, A short history of SHELX, Acta Cryst. A64 (2008) 112-122.

[29] T.A. Halgren, Merck Molecular Force Field. I. Basis, Form, Scope, Parameterization, and Performance of MMFF94, J. Comput. Chem. 17 (1996) 490-519.

[30] Spartan '14 v. 1.1.0. Wavefunction, Inc.: Irvine, CA, USA, 2013.

[31] P. Hohenberg, W. Kohn, Inhomogeneous Electron Gas, Phys. Rev. 136 (1964) B864-B871.

[32] A.D. Becke, Density-functional thermochemistry. III. The role of exact exchange, J. Chem. Phys. 98 (1993) 5648-5652.

[33] C. Lee, W. Yang, R.G. Parr, Development of the Colle-Salvetti correlation-energy formula into a functional of the electron density, Phys. Rev. B 37 (1988) 785-789.

[34] M.J. Frisch, G.W. Trucks, H.B. Schlegel, G.E. Scuseria, M.A. Robb, J.R. Cheeseman, J.A. Montgomery, T. Vreven, K.N. Kudin, J.C. Burant, J.M. Millam, S.S. Iyengar, J. Tomasi, V. Barone, B. Mennucci, M. Cossi, G. Scalmani, N. Rega, G.A. Petersson, H. Nakatsuji, M. Hada, M. Ehara, K. Toyota, R. Fukuda, J. Hasegawa, M. Ishida, T. Nakajima, Y. Honda, O. Kitao, H. Nakai, M. Klene, X. Li, J.E. Knox, H.P. Hratchian, J.B. Cross, V. Bakken, C. Adamo, J. Jaramillo, R. Gomperts, R.E. Stratmann, O. Yazyev, A.J. Austin, R. Cammi, C. Pomelli, J.W. Ochterski, P.Y. Ayala, K. Morokuma, G.A. Voth, P. Salvador, J.J. Dannenberg, V.G. Zakrzewski, S. Dapprich, A.D. Daniels, M.C. Strain, O. Farkas, D.K. Malick, A.D. Rabuck, K. Raghavachari, J.B. Foresman, J.V. Ortiz, Q. Cui, A.G. Baboul, S. Clifford, J. Cioslowski, B.B. Stefanov, G. Liu, A. Liashenko, P. Piskorz, I. Komaromi, R.L. Martin, D.J. Fox, T. Keith, M.A. Al-Laham, C.Y. Peng, A. Nanayakkara, M. Challacombe, P.M.W. Gill, B. Johnson, W. Chen, M.W. Wong, C. Gonzalez and J.A. Pople, Gaussian 03 (Revision C.02), Gaussian, Inc., Wallingford, CT, 2004.

[35] a) P.C. Hariharan, J.A. Pople, The Influence of Polarization Functions on Molecular Orbital Hydrogenation Energies, Theoret. Chim. Acta 28 (1973) 213-222; b) M.M. Francl, W.J. Pietro, W.J. Hehre, J.S. Binkley, M.S. Gordon, D.J. DeFrees, J.A. Pople, Self-consistent molecular orbital methods. XXIII. A polarization-type basis set for second-row elements, J. Chem. Phys. 77 (1982) 3654-3665.

[36] K.T. Givens, S. Kitada, A.K. Chen, J. Rothschiller, D.A. Lee, Proliferation of human ocular fibroblasts. An assessment of in vitro colorimetric assays, Invest. Ophthalmol. Visual Sci. 31 (1990) 1856-1862.

[37] A. Abdullah, F. Huq, A. Chowdhury, H. Tayyem, P. Beale, K. Fisher, Studies on the synthesis, characterization, binding with DNA and activities of two *cis*-planaramineplatinum(II) complexes of the form: *cis*-PtL(NH3)Cl2 where L = 3-hydroxypyridine and 2,3-diaminopyridine, BMC Chem. Biol. 6 (2006) 3.

[38] D.S. Sappal, A.K. McClendon, J.A. Fleming, V. Thoroddsen, K. Connolly, C. Reimer, R.K. Blackman, C.E. Bulawa, N. Osheroff, P. Charlton, L.A. Rudolph-Owen, Biological characterization of MLN944: A potent DNA binding agent, Mol. Cancer Ther. 3 (2004) 47-58.

[39] A. Casini, C. Gabbiani, F. Sorrentino, M.P. Rigobello, A. Bindoli, T.J. Geldbach, A. Marrone, N. Re, C.G. Hartinger, P.J. Dyson, L. Messori, Emerging Protein Targets for Anticancer Metallodrugs: Inhibition of Thioredoxin Reductase and Cathepsin B by Antitumor Ruthenium(II)-Arene Compounds, J. Med. Chem. 51 (2008) 6773-6781.

[40] M.E. Monge, S.M. Bonesi, R. Erra-Balsells, Synthesis and Isolation of Iodocarbazoles. Direct Iodination Reaction of *N*-Substituted Carbazoles, J. Heterocyclic Chem. 39 (2002) 933-941.

[41] a) J.Y. Lee, K.W. Song, H.J. Song, D.K. Moon, Synthesis and photovoltaic property of donor–acceptor type conjugated polymer containing carbazole and 4,7-dithiazolylbenzothiadiazole moiety utilized as a promising electron withdrawing unit, Synth. Met. 161 (2011) 2434-2440; b) T. Wang, Z. Zhang, N.A. Meanwell, J.F. Kadow, Z. Yin, Q.M. Xue, A. Regueiro-Ren, J.D. Matiskella, Y. Ueda, Composition and antiviral activity of substituted azaindoleoxoacetic piperazine derivatives, US. Pat. Appl. Publ. (2004) US 20040110785.

[42] D. Kim, J.K. Lee, S.O. Kang, J. Ko, Molecular engineering of organic dyes containing *N*-aryl carbazole moiety for solar cell, Tetrahedron 63 (2007) 1913-1922.

[43] a) R. Parthasarathy, B. Paul, W. Korytnyk, X-Ray and NMR Studies on Thiazolidines: Crystal Structure and Conformational Equilibria of *N*-Acetyl-2-(*p*-tolyl)thiazolidine-4-carboxylic Acid and Related Thiazolidine Derivatives, J. Am. Chem. Soc. 98 (1976) 6634-6643; b) T. Murai, F. Hori, T. Maruyama, Intramolecular Cyclization of in Situ Generated Adducts Formed between Thioamide Dianions and Thioformamides Leading to Generation of 5-Amino-2-thiazolines and 5-Aminothiazoles, and Their Fluorescence Properties, Org. Lett. 13 (2011) 1718-1721; c) Z.-C. Song, G.-Y. Ma, H.-L. Zhu, Synthesis, characterization and antibacterial activities of *N*-*tert*-butoxycarbonyl-thiazolidine carboxylic acid, RSC Adv. 5 (2015) 24824-24833; d) A.R. Stefankiewicz, A. de Cian, J. Harrowfield, Helix-helix

interactions – homochirality and heterochirality, CrystEngComm 13 (2011) 7207-7211; e) Z.-C. Song, G.-Y. Ma, P.-C. Lv, H.-Q. Li, Z.-P. Xiao, H.-L. Zhu, Synthesis, structure and structure–activity relationship analysis of 3-*tert*-butoxycarbonyl-2-arylthiazolidine-4-carboxylic acid derivatives as potential antibacterial agents, Eur. J. Med. Chem. 44 (2009) 3903-3908.

[44] A. Bondi, van der Waals Volumes and Radii, J. Phys. Chem. 68 (1964) 441–451.

[45] G.R. Desiraju, T. Steiner, The Weak Hydrogen Bond in Structural Chemistry and Biology. IUCR Monographs on Crystallography, vol. 9, Oxford University Press, Oxford, UK, 1999.

[46] a) J. Gu, W.-Q. Chen, T. Wada, D. Hashizume, X.-M. Duan, From supermolecular sheet to helix by breaking molecular symmetry: the case of 4-[2-(carbazol-3-yl)vinyl] pyridium tosylate, CrystEngComm 9 (2007) 541-544; b) P. Xue, B. Yao, J. Sun, Z. Zhang, R. Lu, Emission enhancement of a coplanar π-conjugated gelator without any auxiliary substituents, Chem. Commun. 50 (2014) 10284-10286; c) N.A. Kazin, Y.A. Kvashnin, R.A. Irgashev, W. Dehaen, G.L. Rusinov, V.N. Charushin, Direct arylalkenylation of furazano[3,4-*b*]pyrazines via a new C–H functionalization protocol, Tetrahedron Lett. 56 (2015) 1865-1869; d) J.B. Seneclauze, P. Retailleau, R. Ziessel, Design and preparation of neutral substituted fluorene- and carbazole-based platinum(II)–acetylide complexes, New J. Chem. 31 (2007) 1412–1416.

[47] a) C. López, A. Caubet, S. Pérez, X. Solans, M. Font-Bardía, Easy access to diastereomerically pure platinacycles, Chem. Commun. (2004) 540-541. b) C. López, A. Caubet, S. Pérez, X. Solans, M. Font-Bardía, E. Molins, Chiral Platinum(II) Compounds Containing Ferrocenyl Schiff Bases Acting as (N), $(N,O)^-$, $[C(sp^2,ferrocene),N]^-$ or $[C(sp^2,ferrocene),N,O]^{2-}$ Ligands, Eur. J. Inorg. Chem. (2006) 3974-3984; c) D. Talancón, C. López, M. Font-Bardía, T. Calvet, J. Quirante, C. Calvis, R. Messeguer, R. Cortés, M. Cascante, L. Baldomà, J. Badía, Diastereomerically pure platinum(II) complexes as antitumoral agents. The influence of the mode of binding {(N), $(N,O)^-$ or $(C,N)\}^-$ of (*1S,2R*)–[(η^5-C_5H_5)Fe{(η^5-C_5H_4)–CH═N–CH(Me)–CH(OH)–C_6H_5}] and the arrangement of the auxiliary ligands, J. Inorg. Biochem. 118 (2013) 1-12.

[48] a) M. Crespo, M. Font-Bardía, J. Granell, M. Martínez, X. Solans, Cyclometallation on platinum(II) complexes; the role of the solvent and added base donor capability on the reaction mechanisms, Dalton Trans. (2003) 3763-3769; b) M. Crespo, R. Martín, T. Calvet, M. Font-Bardía, X. Solans, Novel platinum(II) compounds with *N*-benzylidenebenzylamines: Synthesis, crystal structures and the effect of *cis* or *trans* geometry on cycloplatination, Polyhedron 27 (2008) 2603-2611; c) C. López , R. Bosque, M. Pujol, J. Simó, E. Sevilla, M. Font-Bardía, R. Messeguer, C. Calvis, Experimental and Theoretical Studies of the Factors Affecting the Cycloplatination of the Chiral

Ferrocenylaldimine (*SC*)-[(η5-C5H5)Fe{(η5-C5H4)–C(H)═N–CH(Me)(C6H5)}], Inorganics 2 (2014) 620-648.

[49] See for instance: C. López, C. Moya, P.K. Basu, A. González, X. Solans, M. Font-Bardía, T. Calvet, E. Lalinde, M.T. Moreno, Synthesis, crystal structures and properties of *cis*- and *trans*-isomers of [Pt{C6H4-4R1-1-[C8H4N-3'-NOMe]}Cl2(dmso)] (R1 = H or Cl), J. Mol. Struct. 999 (2011) 49-59.

[50] a) F.H. Allen, The Cambridge Structural Database: a quarter of a million crystal structures and rising, Acta Cryst., Sect. B: Struct. Sci. B58 (2002) 380-388; b) Cambridge Crystallographic Data Centre. Available online: www.ccdc.cam.ac.uk/data_request/cif (accessed 15 May 2017).

[51] A. Crosby, J.N. Demas, The Measurement of Photoluminescence Quantum Yields. Review, J. Phys. Chem. 75 (1971) 991-1024.

[52] a) P.D. Leeson, B. Springthorpe, The influence of drug-like concepts on decision-making in medicinal chemistry, Nat. Rev. Drug Discovery 6 (2007) 881-890; b) C.H. Reynolds, B.A. Tounge, S.D. Bembenek, Ligand Binding Efficiency: Trends, Physical Basis, and Implications, J. Med. Chem. 51 (2008) 2432-2438; c) J.A. Arnott, R. Kumar, S.L. Planey, Lipophilicity indices for drug development, J. Appl. Biopharm. Pharmacokinet. 1 (2013) 31-36; d) K.D. Freeman-Cook, R.L. Hoffman, T.W. Johnson, Lipophilic efficiency: the most important efficiency metric in medicinal chemistry, Future Med. Chem. 5 (2013) 113-115.

[53] Selected recent articles on carbazoles as Topoisomerase I or II inhibitors: a) W. Wang, X. Sun, D. Sun, S. Li, Y. Yu, T. Yang, J. Yao, Z. Chen, L. Duan, Carbazole Aminoalcohols Induce Antiproliferation and Apoptosis of Human Tumor Cells by Inhibiting Topoisomerase I, ChemMedChem 11 (2016) 2675-2681; b) M. Bashir, A. Bano, A.S. Ijaz, B.A. Chaudhary, Recent Developments and Biological Activities of *N*-Substituted Carbazole Derivatives: A Review, Molecules 20 (2015) 13496-13517.

[54] For a general overview of the role of Topoisomerases in cancer see for instance: Y. Xu, C. Her, Biomolecules 5 (2015) 1652-1670.

[55] S.P. Fricker, Cysteine proteases as targets for metal-based drugs, Metallomics 2 (2010) 366-377.

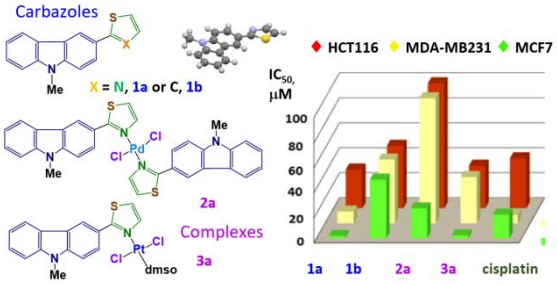

Graphical abstract

Two new N-methylated carbazoles and the Pd(II) and Pt(II) complexes are reported together with a comparative study of their properties, cytotoxic activities (on HCT116, MCF7 and MDA-MB231 cancer cell lines) and their abilities to act as DNA intercalators or inhibitors of cathepsin and Topoisomerases (I or IIα).

HIGHLIGHTS

1. Thiazolyl and thienyl-carbazole derivatives and Pd(II)/Pt(II) complexes are reported

2. The compounds have inhibitory growth effect on HCT116, MDAMB231 and MCF7 cancer cell lines

3. All the compounds are less toxic than cisplatin in the normal and non-tumoral BJ cell line

4. Carbazole **1a** and its Pt(II) complex **3a** are the most potent cytotoxic agents of the series

5. The Pd(II) complex **2a** inhibits the Topoisomerase IIα activity